In presenting the dissertation as a partial fulfillment of the requirements for an advanced degree from the Georgia Institute of Technology, I agree that the Library of the Institute shall make it available for inspection and circulation in accordance with its regulations governing materials of this type. I agree that permission to copy from, or to publish from, this dissertation may be granted by the professor under whose direction it was written, or, in his absence, by the Dean of the Graduate Division when such copying or publication is solely for scholarly purposes and does not involve potential financial gain. It is understood that any copying from, or publication of, this dissertation which involves potential financial gain will not be allowed without written permission.

7/25/68

STUDY OF THE CONTINENTAL STRUCTURE OF SOUTHEASTERN UNITED STATES BY DISPERSION OF RAYLEIGH WAVES

A THESIS

Presented to

The Faculty of the Division of Graduate

Studies and Research

by

Uday Prakash Mathur

In Partial Fulfillment

of the Requirements for the Degree

Master of Science in Geophysical Sciences

Georgia Institute of Technology

September, 1971

STUDY OF THE CONTINENTAL STRUCTURE OF SOUTHEASTERN

UNITED STATES BY DISPERSION OF RAYLEIGH WAVES

Approved:

Chairman

Date approved by Chairman: Aug 27, 1971

ACKNOWLEDGEMENTS

This research was performed under the direction of Dr. L. T. Long, Assistant Professor of Geophysics at Georgia Institute of Technology. I wish to express my gratitude to Dr. Long for his guidance throughout this work, particularly for his many helpful suggestions in analysis of the data and for editing the manuscript.

Deep appreciation is extended to Mineral Engineering Branch of the Chemical Sciences and Materials Division of the Engineering Experiment Station, Georgia Institute of Technology, for the use of equipment and records of the ATL World Wide Standard Seismograph station, and to the Seismological Data Center, Asheville, North Carolina, for supplying negative film copies of the long period seismograms for all the earthquakes.

During my tenure as a graduate student in the School of Geophysical Sciences, I was awarded a Research Assistantship supported by the National Science Foundation (Grant Number GA-012391) and was also employed part-time by the Mineral Engineering Branch of the Engineering Experiment Station. The experience that I gained during my employments enhanced my knowledge of seismology and contributed to work on this thesis.

TABLE OF CONTENTS

LIST OF TABLES

LIST OF FIGURES

LIST OF FIGURES (Concluded)

ABSTRACT

Phase velocity dispersion curves for fundamental mode Rayleigh waves are calculated for the portion of the Southeast United States between the Atlantic Coastal Plain and the Appalachian Plateau. Four WWSSN stations (ATL, SHA, OXF, and BLA), which fall within this area, were used.

The arrival times of the various phases were smoothed and then fitted to a linear epicentral distance versus arrival time curve by the method of least mean squares. The effects of curvature and diffraction, at different periods, were accounted for by computing the standard deviation of the least mean squares fit for "false" epicenters. Phase velocities were then calculated for periods from 20 seconds to 45 seconds by the method of least squares from the "false" epicenter which gave minimum standard deviation.

The dispersion curves showed little variation throughout the area, indicating a uniform crustal structure. By comparison to theoretical dispersion curves a crustal model consisting of four layers with shear wave velocities of 3.30 km/sec, 3.47 km/sec, 3.58 km/sec, 3.75 km/sec and 4.56 km/sec, and thicknesses of 1 km, 15 km, 15 km, and 10 km (total crustal thickness of 41 km) was considered the best fit. However, a number of models with velocity of 3.34 km/sec in the upper crust increasing to 3.75 km/sec in the lower crust could satisfy the observed data.

The crustal thickness of 41 km is consistent with an analysis of unreversed travel times in the Southeast United States. The refraction analysis indicates a velocity structure consisting of a 5.3 km layer with shear and compressional wave velocity of 3.21 km/sec and 5.77 km/sec

respectively over a 34.7 km thick lower crustal layer with shear and compressional wave velocities of 3.78 km/sec and 6.75 km/sec respectively.

INTRODUCTION

The velocity-depth structure of the upper regions of the earth can be determined by the analysis of the dispersion of seismic surface waves. Depths to the different seismic discontinuities and velocities cannot be as accurately evaluated by other geophysical methods such as gravity, magnetic, and electrical measurements. The seismic refraction methods are difficult to apply to shear waves and are not capable of identifying low velocity layers or small velocity contrasts.

There are essentially two types of surface waves, Rayleigh and Love. Rayleigh waves require only a free surface for propagation and have an elliptical retrograde partical motion in the vertical plane. Love waves are horizontally polarized shear waves, which require a free surface and a lower velocity surface layer for propagation. The dependence of velocity of these surface waves on wave length (or frequency) constitutes dispersion. The theory of surface wave propagation shows that dispersion depends on the velocity structure of the medium through which the Rayleigh and Love waves propagate. The seismic surface waves with longer periods are affected by the deeper, higher-velocity mantle and hence arrive earlier than the shorter waves travelling with velocities more representative of shallower layers. Dispersion also provides a means of detecting the presence of lower velocity layers at depth (if they exist).

Two principle methods that can be used to study surface wave dispersion are the group velocity method and the phase velocity method. The group velocity method uses velocity of energy propagation whereas the

phase velocity measurement method utilizes two or more seismic stations to determine velocity of a crest (or phase) between them. The chief purpose of this study is to determine the velocity depth distribution in a portion of Southeast United States by measuring phase velocities between four Worldwide Standard Seismograph stations (ATL, BLA, OXF, and SHA). The measured dispersion is compared to theoretical dispersion curves to find the most likely velocity structure for the area bounded by the four stations. A final crustal model is then constructed which is found to be consistent with previously published work and observed travel times.

LITERATURE

Crustal Structure in Southeast United States

Among the earliest seismic refraction work performed in the central and southern portions of the Eastern United States was that of Tatel et al. (1953), Tuve et al. (1954), and Tatel and Tuve (1966). Since these early studies, little additional work has been published in delineating the structure of the crust and upper mantle in this region. Studies of shallow crustal structure were undertaken by Skeels (1950), Bonini (1957), and Meyer (1955). Off-shore investigations were carried out by Ewing and Press (1950) and Harsey et al. (1959).

The TVA shots fired at South Holston Dam in northeastern Tennessee during 1950 were observed to the northeast along the strike of the Appalachian structure and to the northwest and southeast, normal to the axis of the mountains. An interpretation of Tatel et al. (1953) of arrivals to a distance of 360 km indicated that the crust at South Holston Dam is about 45 km thick with a mean crustal velocity of 6.57 km/sec, the mantle velocity was found to be 8.06 km/sec. The crustal model as suggested by Stienhart and Meyer (1961) for eastern Tennessee (h_1 = 13.7 km, h_2 = 31.6 km, V_1 = 6.20 km/sec, V_2 = 6.73 km/sec, V_3 = 8.06 km/sec) matches well with Tatel's (1953) results as given above. Bollinger (1970) in the study of central Appalachian earthquakes obtained the following velocities: Sg = 3.60 km/sec, Sn = 4.32 km/sec and Pn = 8.10 km/sec for the southeastern United States.

Warren et al. (1966) reported on a refraction survey to determine the

crustal structure in southern Mississippi along a line trending north from Ansley to Oxford. The most reliable results were from the part of the survey between Ansley and Raleigh, where they had a reversed refraction-line coverage. Their crustal structure interpretation (see Figure 1) consisted of a surface layer of 5.0 km/sec down to a depth of 3.1 to 3.7 km overlying the upper crystalline crust of 5.9 km/sec velocity and having thickness of 6 km at Ansley and 10 km at Collins. The velocity of the lower crust was measured as 6.9 km/sec; the surface of the lower crust was found to be dipping 2^{o} S between McNeill and Collins. Computed thickness was 19 km at McNeill and 13 km at Raleigh. A dip of 3^{o} S on the top of the mantle was measured, using strong events interpreted as reflection from the M Discontinuity to supplement the weak P_n first arrivals. The computed depth to the top of the mantle was 41 km at Ansley and 29 km at Raleigh. The velocity in the upper mantle was found to be 8.4 ± 0.3 km/sec.

The structure in and around the Blake Plateau is complex, and Harsey et al. (1959) have suggested that there is a deep sediment-filled trough roughly parallel to the coast. This trough may be continuous with the eastern-most of the two roughly parallel sediment-filled trenches found by Drake et al. (1959) at the foot of the continental rise of Cape Hateras.

A cooperative seismic crustal structure experiment (Hales et al., 1968), involving eleven participating institutions including Georgia Tech, was conducted off the east coast of the United States during the summer of 1965. The analysis of the data for the southern profiles indicated a crustal structure of 0.49 km of sediments (1.7 km/sec) overlying 30.38 km of basement (6.03 km/sec) and a mantle velocity of 8.13 km/sec. The northern profiles indicated 1.63 km of sediment (2.10 km/sec) above 8.31 km

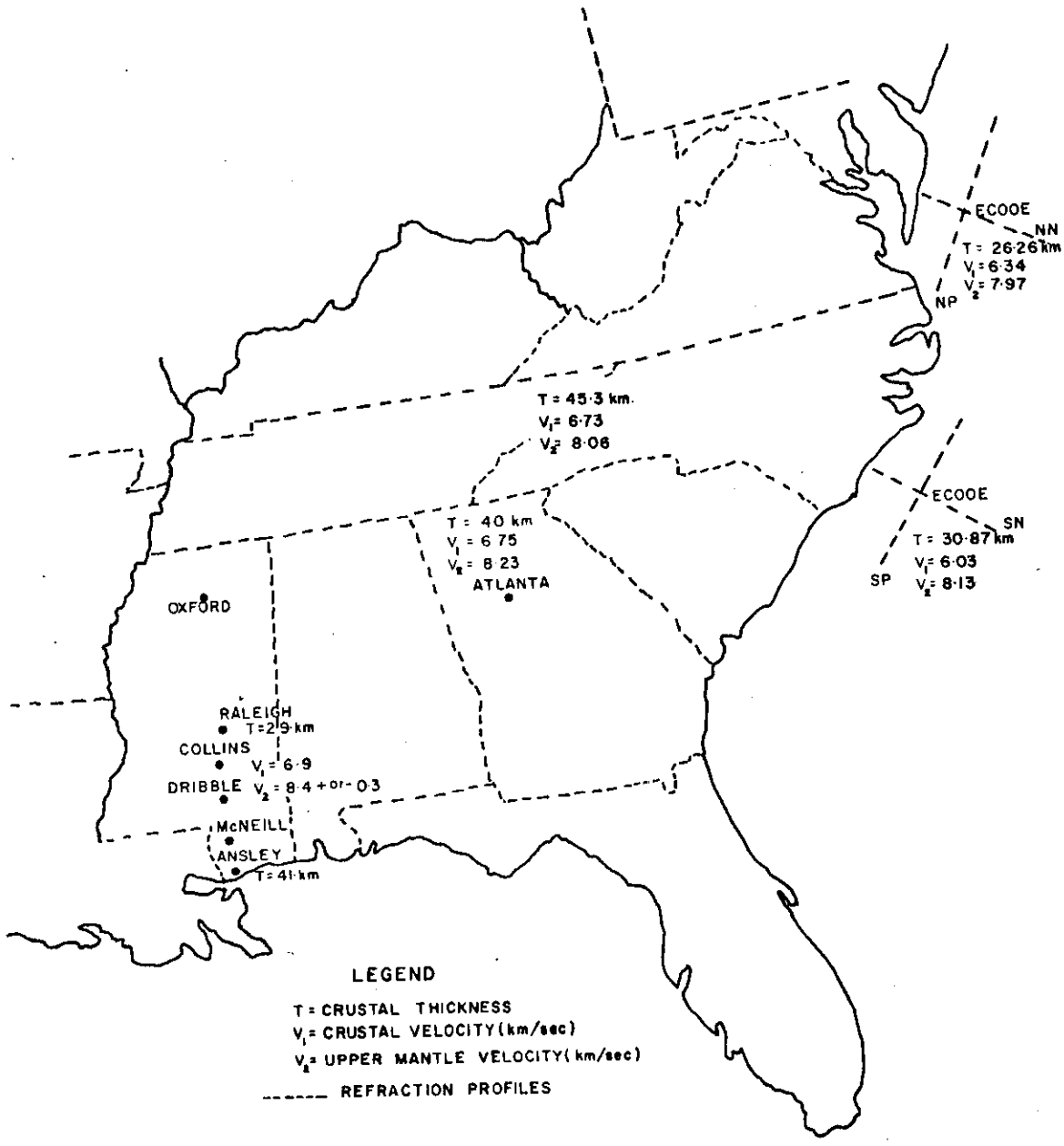

Figure 1. Map Showing the Previous Work Done in and Around the Area of Study.

of upper crust (5.78 km/sec) and 16.32 km of lower crust (6.34 km/sec) and a mantle velocity of 7.97 km/sec.

In 1970, the author did a travel time analysis (as a special project) using five Georgia quarry blasts and four local earthquakes in the southeastern United States. The crustal structure estimated for the area surrounding the ATL observatory (i.e. portions of Georgia, Tennessee, Alabama, South Carolina, and North Carolina (see Figure 1)) consists of three layers (h_1 = 5.31 km, h_2 = 34.7 km, V_1 = 5.77 km/sec, V_2 = 6.75 km/sec, V_3 = 8.23 km/sec, V_{s1} = 3.2 km/sec, V_{s2} = 3.78 km/sec. The data of this study are discussed in Appendix I.

Surface Wave Dispersion

Gutenberg (1924) was among the first to investigate crustal structure by using the dispersion of surface waves. Later with increased observations and with improved computational techniques numerous analyses have been made on the dispersion of surface waves and their relation to crustal and subcrustal structures in various regions.

Wilson and Baykal (1948) studied Rayleigh wave group-velocity dispersion across the Atlantic Ocean and were among the first to make corrections for the continental portion of the path traveled. A single surface layer was assumed for the crustal model while attempting to explain observed dispersion.

Evernden (1953, 1954) investigated the technique of using tripartite arrays to determine phase-velocity dispersion of Rayleigh waves. Although he was primarily concerned with the directions of approach of the surface waves, his results were consistent with known structural relationships in the area of study. He showed that the phase-velocity dispersion

measurements could be obtained when separate phases in a Rayleigh wave train are correlated across a tripartite array.

Press (1956) used the tripartite method to determine the crustal structure from the dispersion of Rayleigh waves. He found the crustal thicknesses in southern California by comparing the observed dispersion data with corresponding average curves (phase velocity-period) for the crustal structure in Africa (Press, Ewing, and Oliver, 1956).

Several other regions have been studied since then, using the phase-velocity dispersion of surface waves. Chiburis (1965) determined the crustal structure in the Pacific Northwest states and Payo (1965) investigated the elastic parameters of the crust of the Iberian Peninsula. So far no studies have been reported of the crustal structure of the Southeast United States by using the phase-velocity dispersion technique.

STRUCTURAL PROVINCES IN THE SOUTHEASTERN UNITED STATES COVERING THE AREA OF INVESTIGATION

The index map of Figure 2 shows the main structural divisions in the Southeastern United States (after Eardley, 1962). Most of the phase velocity dispersion observations were taken at stations along the regional strike or just east of the Appalachian Plateaus.

The Appalachian Plateau Province lies on the eastern margin of what is called the central stable region. The strata of the Appalachian Plateau are nearly horizontal and do not show evidence of structural deformation after deposition during the Paleozoic era.

The folded and thrust-faulted Appalachian Mountains, east of the Appalachian Plateaus, consist of flat-topped, almost parallel ridges and valleys. They are carved out of anticlines, synclines and thrust sheets. The strata were implaced during the Paleozoic Era in both provinces, but thicken from the shelf along the western margin of the plateau to the geosyncline in the eastern part of the plateaus and in the folded and thrust-faulted belt.

The Blue Ridge province consists of Cambrian and Precambrian metamorphic and igneous rocks. The widest portion is in the south and the highest is in the Great Smoky Mountains of Tennessee and North Carolina. The Blue Ridge province is generally one of conspicuous relief east of the Great Valley of the folded Appalachians and west of the crystalline Piedmont. The Piedmont province is broad and generally of low relief. Its rocks are not well exposed and are, as yet, thoroughly known in only

Figure 2. Index Map of the Structural Systems of the Eastern Margin of the Continent.

a few places. They are chiefly metamorphosed Precambrian and Paleozoic sedimentary and volcanic sequences which include Paleozoic plutons, a number of which are of batholithic proportions.

The Atlantic Coastal Plain is a continuation of the Gulf Coastal Plain, and is made up of Cretaceous and Tertiary sediments that rest unconformably on the older rocks of all the structural system of the Appalachian Mountains.

DISCUSSION OF METHODS

There are basically two methods of measuring the velocities of dispersive surface waves. One measures the group velocity, U, of these waves by making use of the relation

$$U(K) = D/t(K)$$

where D is the epicentral distance and t(k) is the travel time from epicenter to station of surface wave energy with period K. This method provides information of the composite structure between the epicenter and the recording station. For sufficient resolution of the crustal structure, the source and the station should preferably be within similar geologic provinces. It is also important that there is sufficient dispersion of the longer periods so as to determine deeper structures. The limited extent of the crustal structure typical in the Southeast United States and sparsity of the events make this method unsuitable.

The second method utilizes time differences of separate phases in the surface-wave train between close stations to calculate phase velocities. One technique is to determine both direction of approach and phase velocity with a tripartite array (three non-colinear recording stations). The results obtained by using this method were often unreliable and the phase velocities were found to vary considerably. The scatter could be because the triangle ATL, BLA, SHA is too narrow to satisfy the requirements of the tripartite method, which assumes that the internal angles are at least 10° to 20° for the resolution of azimuth. In this case, the internal

angles at BLA and SHA were less than 6°. In a nearly linear triangle slight errors in measuring time caused by interfering signals of higher frequencies (noise) or higher modes of the surface waves produce large errors in azimuth and hence large errors in phase velocity. Curvature of wave fronts across the larger arrays, because of diffraction and/or deviation from the plane geometry assumed, leads to errors in the interpretation of arrival times and hence errors in azimuth and phase velocity.

To avoid these difficulties a least squares method was developed to relate arrival times to epicentral distances (assumed linear across the array). This method requires fitting a straight line through two or more points corresponding to the stations used (see Figure 3 a). The inverse of the slope of this line gives phase velocity for each phase considered.

A linear relation is assumed for a set of observed epicentral distances (D_i) and travel times (t_i) from a single event (see Figure 3),

$$t_i = aD_i + C \tag{1}$$

where a is the slope of the straight line and C is the intercept time. The above equation can be easily solved for a and C as follows:

Writing the above equation in matrix form,

$$\begin{bmatrix} t_1 \\ t_2 \\ \cdot \\ \cdot \\ \cdot \\ T_N \end{bmatrix} = \begin{bmatrix} D_1 & 1 \\ D_2 & \\ \cdot & \\ \cdot & \\ \cdot & \\ D_N & 1 \end{bmatrix} \begin{bmatrix} a \\ C \end{bmatrix}$$

(a)

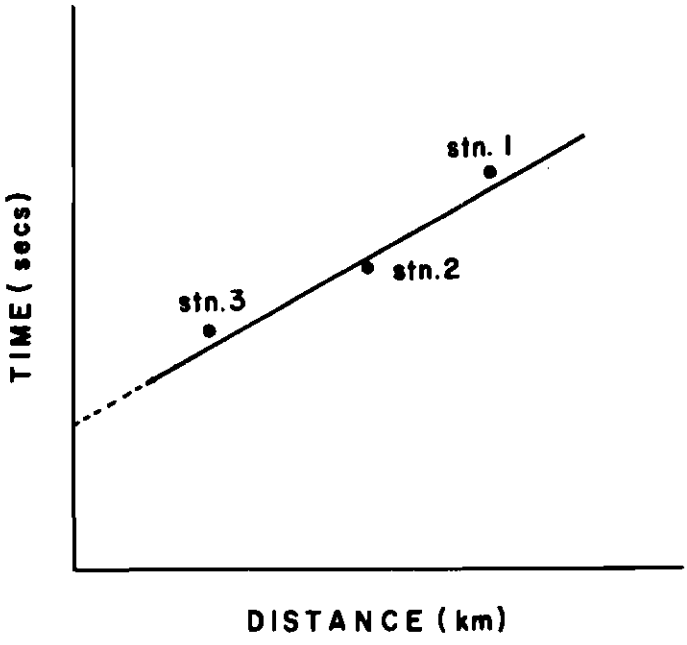

(b)

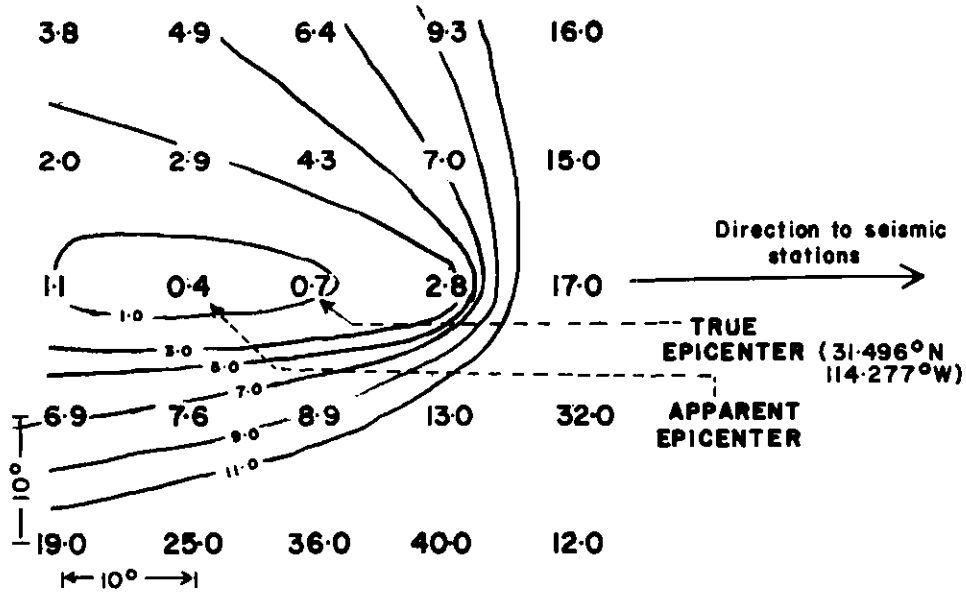

Figure 3. (a) An Example of Least Mean Squares Fit of Arrival Times to Epicentral Distances.
(b) Outline of the Measures of Uncertainty as a function of Latitude and Longitude.

Multiplying both sides by the transpose of the matrix on the right hand side above gives

$$\begin{bmatrix} \Sigma D_i^2 \\ \Sigma D_i \end{bmatrix} \begin{bmatrix} \Sigma D_i \\ N \end{bmatrix} \begin{bmatrix} a \\ C \end{bmatrix} = \begin{bmatrix} \Sigma D_i t_i \\ \Sigma t_i \end{bmatrix}$$

where the summation is taken from i = 1 to N, the number of stations. Calculating the inverse of the left hand matrix and carrying out the multiplication gives

$$\begin{bmatrix} a \\ C \end{bmatrix} = \frac{1}{[N \Sigma D_i^2 - (\Sigma D_i)^2]} \begin{bmatrix} N & - \Sigma D_i \\ \Sigma D_i & \Sigma D_i^2 \end{bmatrix} \begin{bmatrix} \Sigma D_i t_i \\ \Sigma t_i \end{bmatrix}$$

Thus, the solution for C and 1/a (the velocity v) is given as

$$C = \frac{(\Sigma D_i)(\Sigma t_i) - (\Sigma D_i)(\Sigma D_i t_i)}{N \Sigma D_i^2 - (\Sigma D_i)^2}$$

$$v = \frac{1}{a} = \frac{N(\Sigma D_i^2) - (\Sigma D_i)^2}{N(\Sigma D_i t_i) - (\Sigma t_i)(\Sigma D_i)}$$

Also, measures of uncertainty (errors) as given by Bullen (1963, p. 196) can be expressed as

$$E_K = \sqrt{\frac{N \Sigma [(D_i/V)] + C - T_{ik}]^2}{[N(\Sigma D_i^2) - (\Sigma D_i)^2](N-2)}}$$

where K is the period and E_K is the error function.

The measure of uncertainty (E) is then examined as a function of "false" epicenters and an apparent epicenter determined from the minimum E at each frequency. Errors introduced by curvature and refraction are thus minimized. The minimum of E is found by generating twenty four "false" epicenters around the true epicenter in the form of a grid with a spacing of 10 degrees in latitude and longitude. The phase velocities versus period calculated using the apparent epicenter are then used for the evaluation of the crustal structure. To expedite the analysis, computer programs were written to calculate periods, corresponding arrival times, phase velocities, errors and apparent epicenters. The computer program is described in Appendix II.

ANALYSIS

Recording Stations and Earthquakes Used

Four recording stations ATL, BLA, OXF, and SHA were used in this study. All four of them are members of World Wide Standard Seismograph Network (WWSSN). A number of other seismic stations (Figure 4) exist in the Southeast United States; CPO, CHC, ORT, and Fernbank. Recordings from them were not used because they either do not operate instruments appropriate for this study or have insufficient calibration or timing.

Pertinent station information is listed in Table 1. Location of the stations are shown in Figure 4, where the lines connecting the stations are used to indicate generally the extent of the area which is being sampled by the phase velocity determination.

Rayleigh waves recorded from sixteen teleseisms were considered for analysis. Of these only eight were found to be suitable in terms of recording amplitude, for the determination of the phase velocity dispersion in this region. The selected shocks with their corresponding code numbers are listed in Table 2.

Procedure

Since the records used were those of the long-period seismographs (Figure 5) having the same characteristics, phase shift corrections were not applied. Therefore, the phase velocity was obtained directly from the differences in epicentral distance and the arrival times assigned to each crest and trough. Since an error of one cycle leads to obviously erroneous values of phase velocities at longer periods, the initial long period

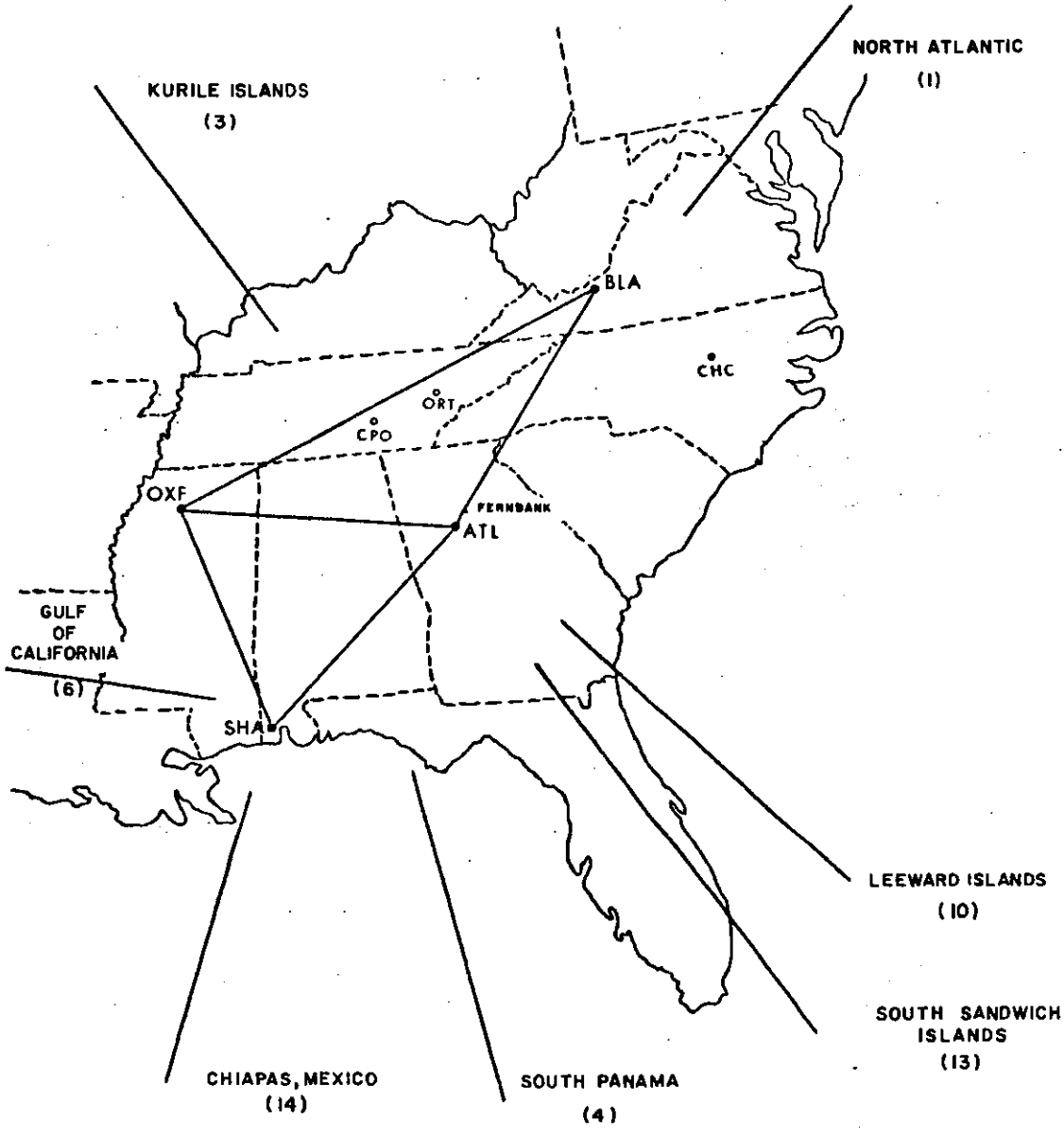

Figure 4. Map Showing the Distribution of Stations and Direction of Approach of Events Used for Analysis.

Table 1. Worldwide Standard Seismograph Network Information

STATION	SYMBOL	LATITUDE	LONGITUDE
Atlanta, Georgia	ATL	33.433° N	84.338° W
Blacksburg, Virginia	BLA	37.211° N	80.421° W
Springhill, Alabama	SHA	30.695° N	88.140° W
Oxford, Mississippi	OXF	34.512° N	89.409° W

Table 2. List of the Distant Earthquakes Considered

No.	Date	Origin Time	Latitude	Longitude	Location
1.	20, Sept., 1969	05:08:57.57	58.297° N	32.189° W	North Atlantic
2.	16, July, 1969	08:16:53.27	52.203° N	158.982° N	East Coast of Kamchatka
3.	13, June, 1969	08:48:29.54	49.442° N	155.495° E	Kurile Islands
4.	25, April, 1969	03:34:17.74	7.450° N	82.075° W	South of Panama
5.	4, April, 1969	16:16:17.20	24.365° N	109.760° W	Gulf of California
6.	28, March, 1969	15:19:40.44	31.496° N	144.277° W	Gulf of California
7.	1, May, 1970	08:35:24.17	14.635° N	93.158° W	Coast of Chiapa, Mexico
8.	6, Jan., 1970	12:56:05.87	15.817° N	59.708° W	Leeward Islands
9.	5, Feb., 1970	22:05:58.34	12.598° N	122.117° E	Luzon, Philippines
10.	7, Jan., 1970	07:56:11.10	15.881° N	59.727° W	Leeward Islands
11.	9, April, 1970	16:24:31.01	13.212° N	92.259° W	Chiapas, Mexico
12.	29, April, 1970	21:20:24.06	14.566° N	93.576° W	Chiapas, Mexico
13.	20, May, 1970	20:23:42.25	55.890° S	28.328° W	South Sandwich Islands
14.	15, May, 1970	09:44:45.23	14.512° N	92.811° W	Chiapas, Mexico
15.	24, May, 1970	10:35:22.09	21.981° N	126.682° E	Western Australia
16.	1, May, 1970	08:35:24.17	14.635° N	93.158° W	Chiapas, Mexico

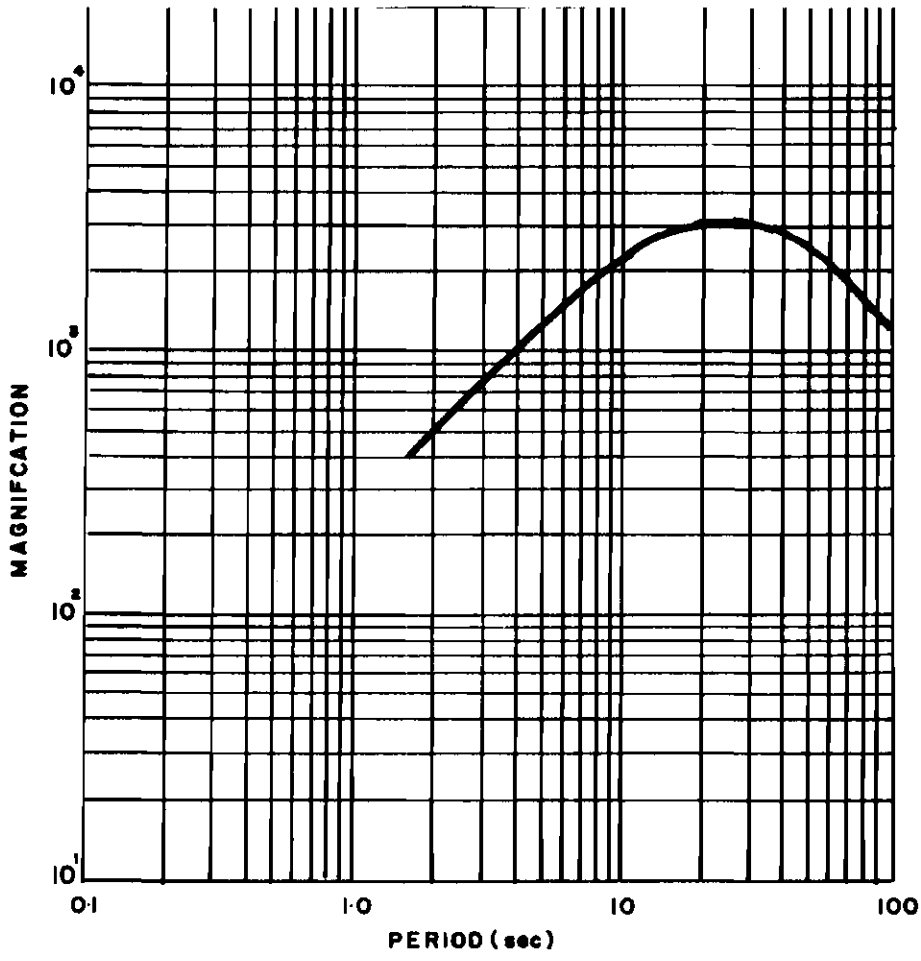

Figure 5. Displacement Response for Long Period (WWSSN) Seismograph.

phases were used to correlate the phases of the events recorded at different stations.

At each station in an array the correlated phases were consecutively numbered and the corresponding arrival times read off the seismograms. The arrival time data were then adjusted by using a smoothing filter (Shipero, 1970). The effects of this filter on phase velocities are shown in Figure 6. Periods were calculated directly from adjusted arrival time data and averaged for the stations used. Phase velocities and estimated errors were then calculated by Least Mean Squares for all periods measured. The errors were found to be large in some cases probably because the refraction of the wave fronts was significant. To overcome this problem other curvatures were considered by generating "false" epicenters and minimum deviations calculated at each, for certain chosen periods. If the deviations "zero in" at the true epicenter it means that the errors in phase velocity were minimum for all phases and there was very little (if at all) refraction of seismic waves from that direction. Phase velocities and errors (for certain chosen period) were then calculated as before for each "false" epicenter having minimum deviation. The final crustal structure was based on the corrected dispersion data that gave good results and had very low errors in phase velocity.

Discussion

Although the phase velocity dispersion method used in this investigation does not give a unique solution of crustal structure, the theoretical models (shown in Appendix III) used for comparison are believed to be realistic approximations because of the physical constraints used. Phase velocity dispersion curves for various line segments, triangles, false

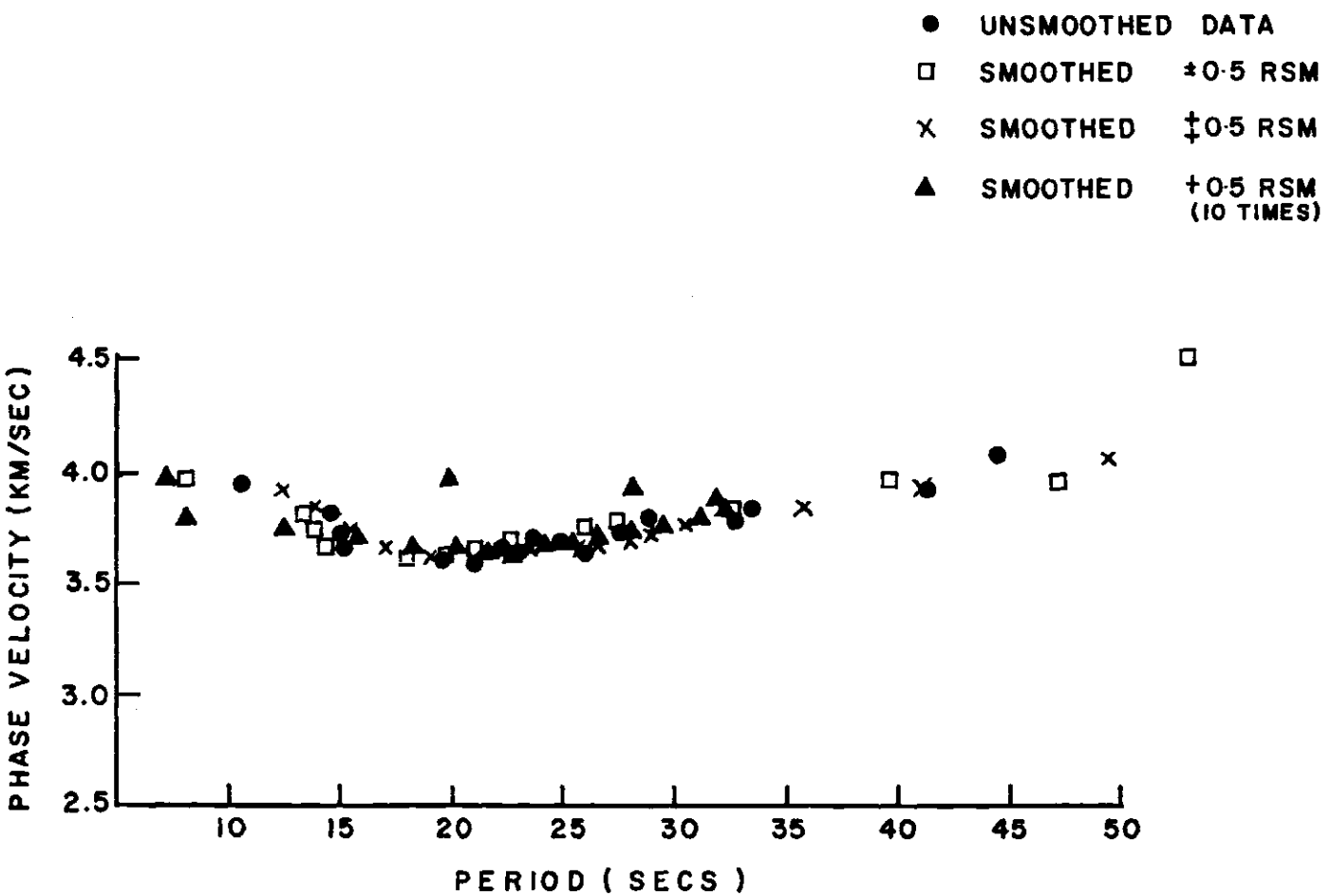

Figure 6. Effect on Smoothing by Different Operations on the Dispersion Data from the California Event (No. 6).

epicenters and a final composite are plotted in Figures 7 to 18.

Phase Velocities of Rayleigh Waves Between SHA and OXF.

The records of the earthquakes which have code numbers 3, 13, and 14 in Table 2 were used to determine phase velocities of Rayleigh waves along this path. It was observed that the short period phases from South Sandwich Islands showed large scatter probably due to the waves refracting around the South American continent and then again at the boundary of the North American continent and the Gulf of Mexico. The longer period 'mantle' velocities, however, are not affected significantly and thus they can be used more reliably in the construction of a phase velocity dispersion curve for the line segment SHA and OXF. The data from Kurile Islands and Chiapas, Mexico, do not show as much scatter, except at the higher frequencies which can be accounted for by the refraction of "some" phases more than others at "lower" periods. Most of the data from the Kurile Islands, Chiapas, Mexico and the South Sandwich Islands at longer periods show a trend along which a dispersion curve is plotted (Figure 7). The observations that were far away from this central line were finally deleted as non-representative of the true phase velocity for corresponding periods. All the observations are shown in Figure 7.

The proper model was chosen by trial and error to fit the observed phase velocity dispersion. Several models, differing only in respect to the thickness of each layer were found to satisfy the data. The one that was most consistent between periods of 18 to 45 seconds, had a crustal thickness of 41 Km.

Rayleigh Waves Between ATL-OXF.

The three earthquakes with code numbers 3, 10, and 13 were considered

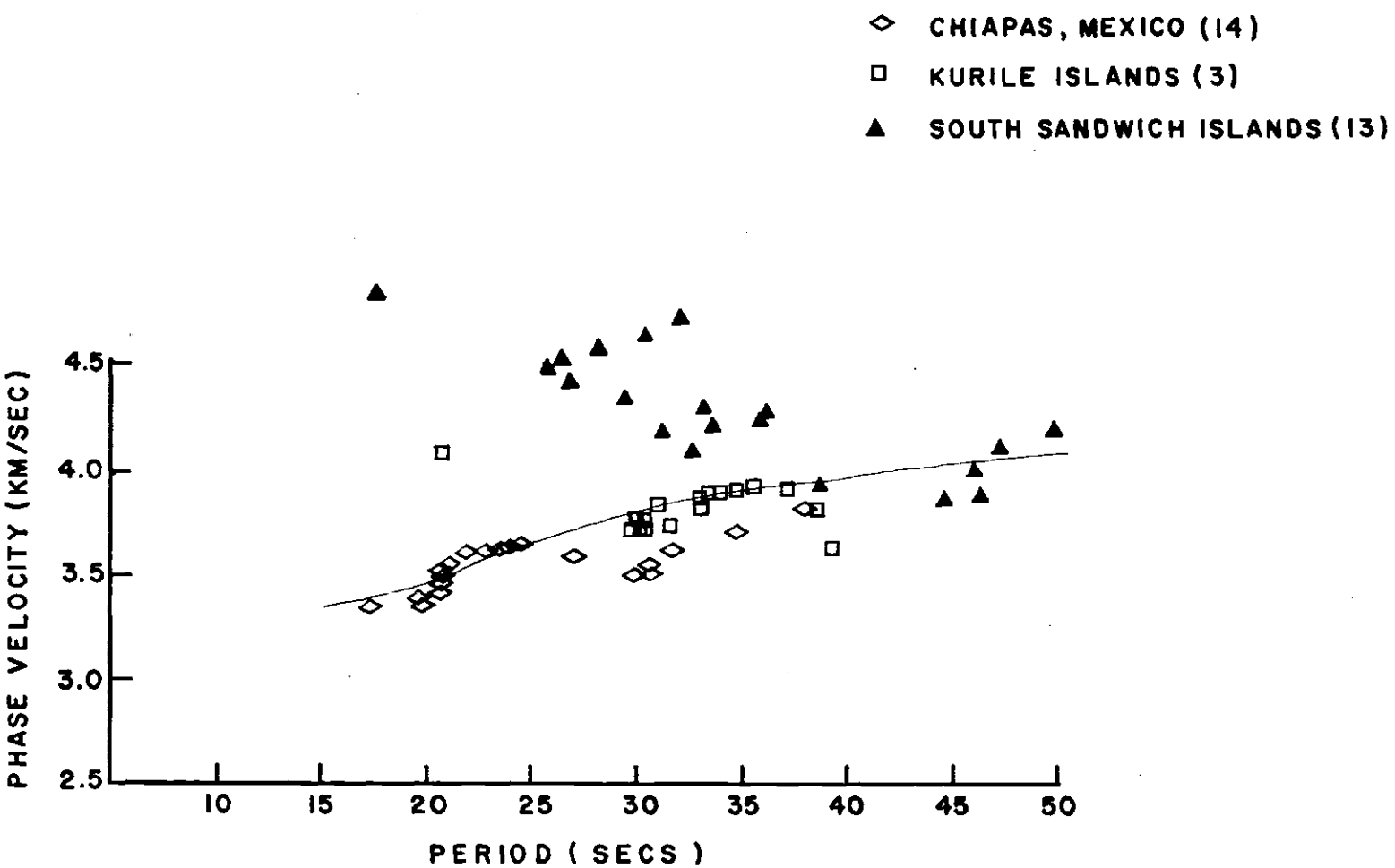

Figure 7. Phase Velocities of Rayleigh Waves Between OXF-SHA.

the most suitable. However, the direction of approach for events 3 and 13 were 47° and 38° respectively to the ATL-OXF line. These angles are too large to give good results because the arrival time differences being small would change the velocities drastically with a slight error in measuring the times (see Figure 8 for scatter for events 3 and 13). Since the higher frequency phases from South Sandwich Islands undergo refraction around South America, the data are unrealistic between periods of 25 secs to 40 secs. Long period (> 40 sec) phases traveling with velocities characteristic of the upper mantle are not affected as much and seem to fall in place if a curve is estimated through the more realistic parts of the data. At the shorter periods the data from Leeward Islands (which deviates only 17° from direct path) is reasonable and smooth. The recorded phase velocities from Kurile Islands show a large scatter at all periods. The scatter is mainly due to the almost normal (Figure 4) direction of approach. An average curve is constructed primarily by the Leeward Islands event and averaging the points at the larger periods (> 40 sec) which are more reliable than the ones between 25-40 sec periods.

The final observed dispersion data are then compared with the theoretical models. The errors are such that several models satisfy the observed dispersion, all indicating a crustal thickness around 42 km. The three theoretical curves that fit the data best are perhaps Nos. 2, 3, 4. They show that the thickness of the crust is of the order of 45 km which compares very well with that obtained by Tatel et al. (1953) just north of the South Holston Dam in Tennessee.

Phase Velocities of Rayleigh Waves Between OXF and BLA.

This section has been included to illustrate the importance of requiring the seismic ray paths to be along or at least close to the line

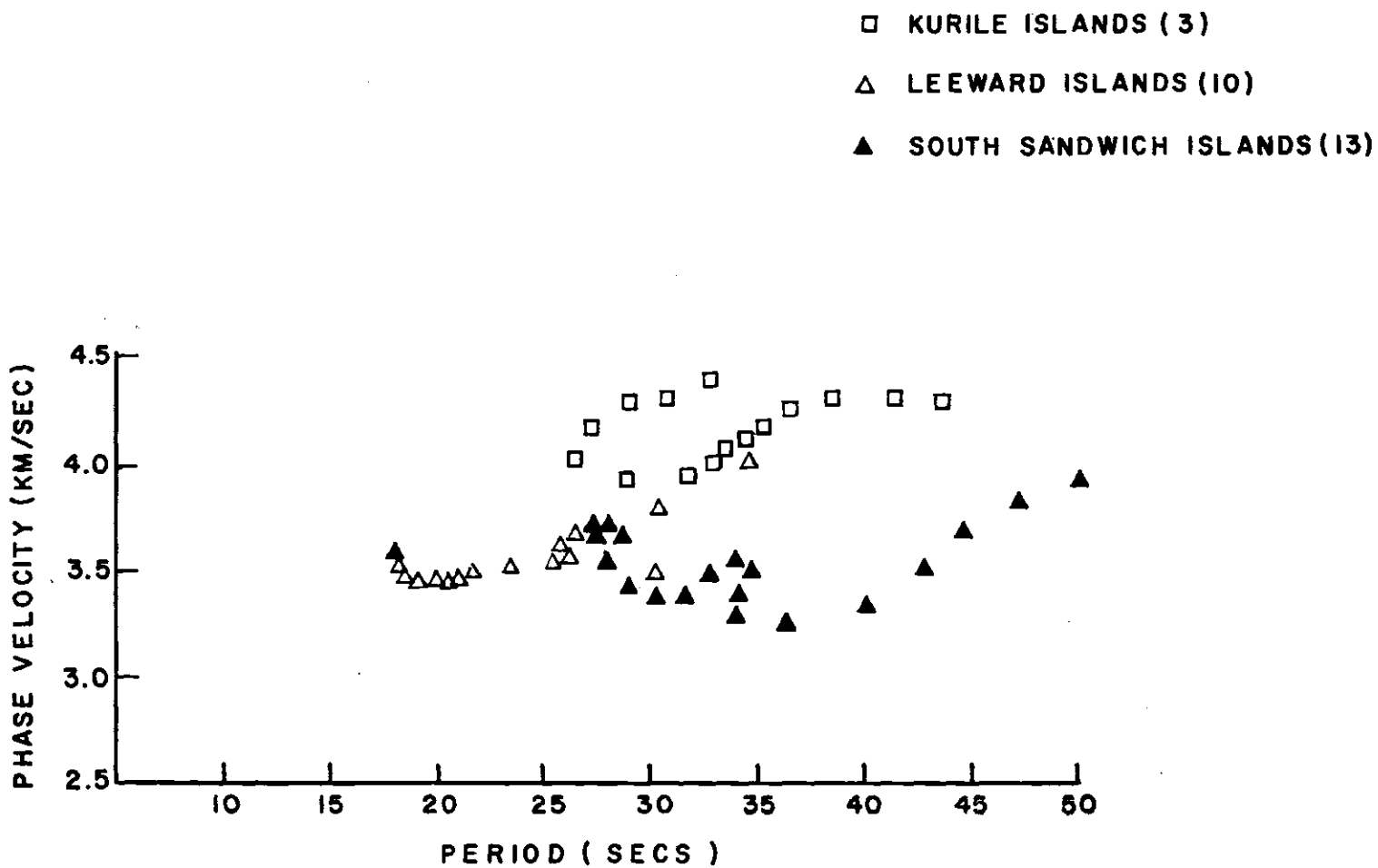

Figure 8. Phase Velocities of Rayleigh Waves Between ATL-OXF.

joining the seismic stations. Data from only two earthquakes 10 and 14 were available for the path between OXF and BLA. Since the direction of approach of Rayleigh waves from Leeward Islands (10) is almost at right angles, it is impossible to find any significant difference in the arrival times for the phases at the two stations. Waves coming from Chiapas, Mexico (14) after refracting from the continental boundary also tend to arrive almost perpendicular to the two stations. Figure 9 thus clearly illustrates the poorly defined dispersion curve as recorded for Rayleigh waves from Chiapas, Mexico.

Phase Velocities of Rayleigh Waves Along the Line BLA-ATL-SHA.

The long-period vertical-component records at the stations BLA, ATL, and SHA of the four earthquakes with code numbers 1, 4, 6, and 14 were used to determine phase velocities as a function of period along this path. In the case of the earthquake with code number 1, the waves traveled the path in the direction of BLA to SHA and in the case of events 4 and 14 the waves traversed the path in the direction of SHA to BLA. In order to determine whether a difference exists the phase velocities of the waves traveling along the segments SHA-ATL-BLA, ATL-BLA, and SHA-ATL were plotted separately in Figures 10, 11, and 12 respectively.

The average velocity errors for all four earthquakes 1, 4, 6, and 14 are respectively 0.28 km/sec, 0.52 km/sec, 0.29 km/sec, and 0.46 km/sec. The errors are tolerable, but for the event from south Panama (4), they are a little high. This is probably because the surface waves strike the continental margin obliquely (Figure 4) resulting in large refraction.

The false epicenter method of focusing could not be used effectively to reduce the errors and improve the velocities because the three stations

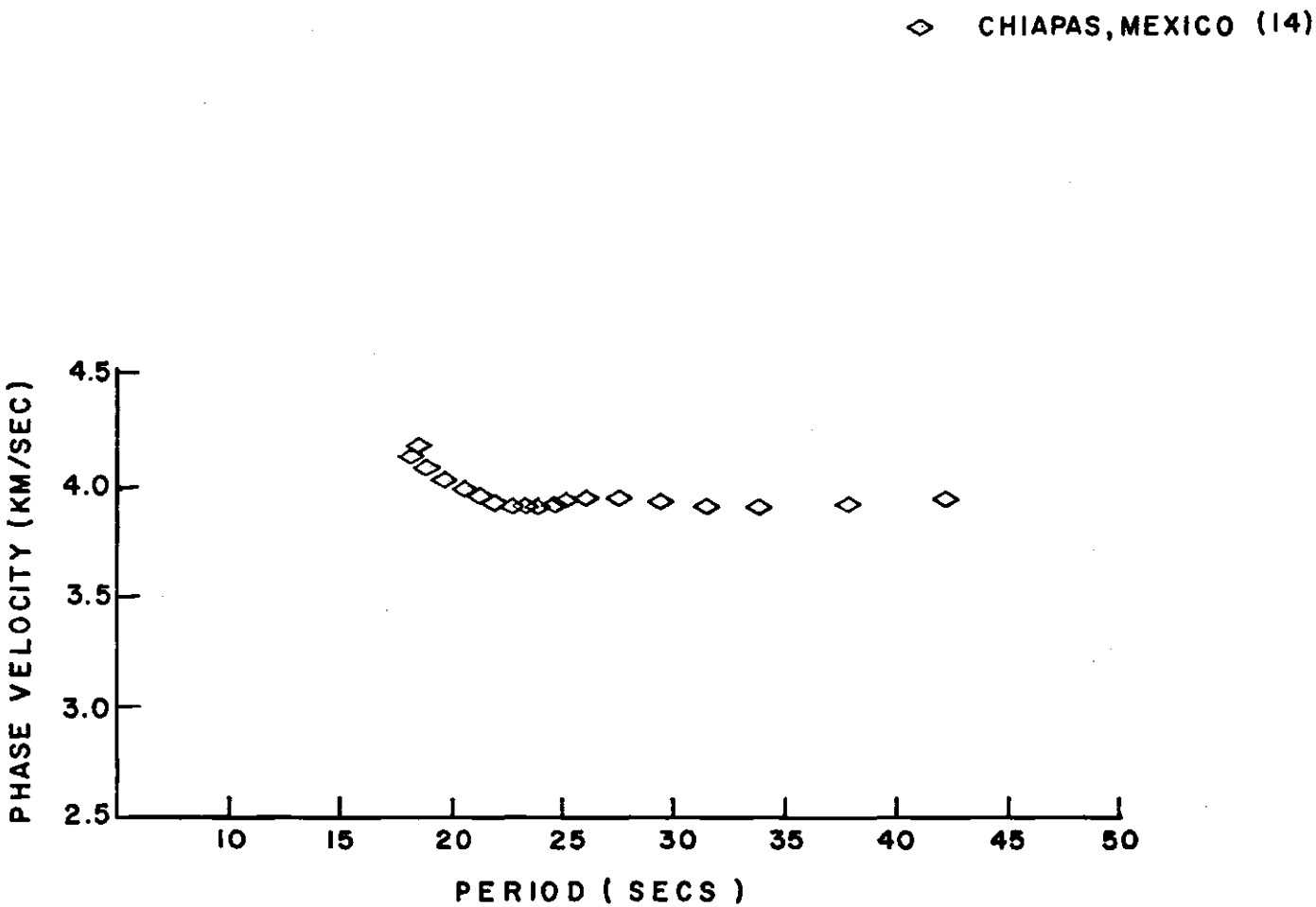

Figure 9. Phase Velocities of Rayleigh Waves Between OXF-BLA.

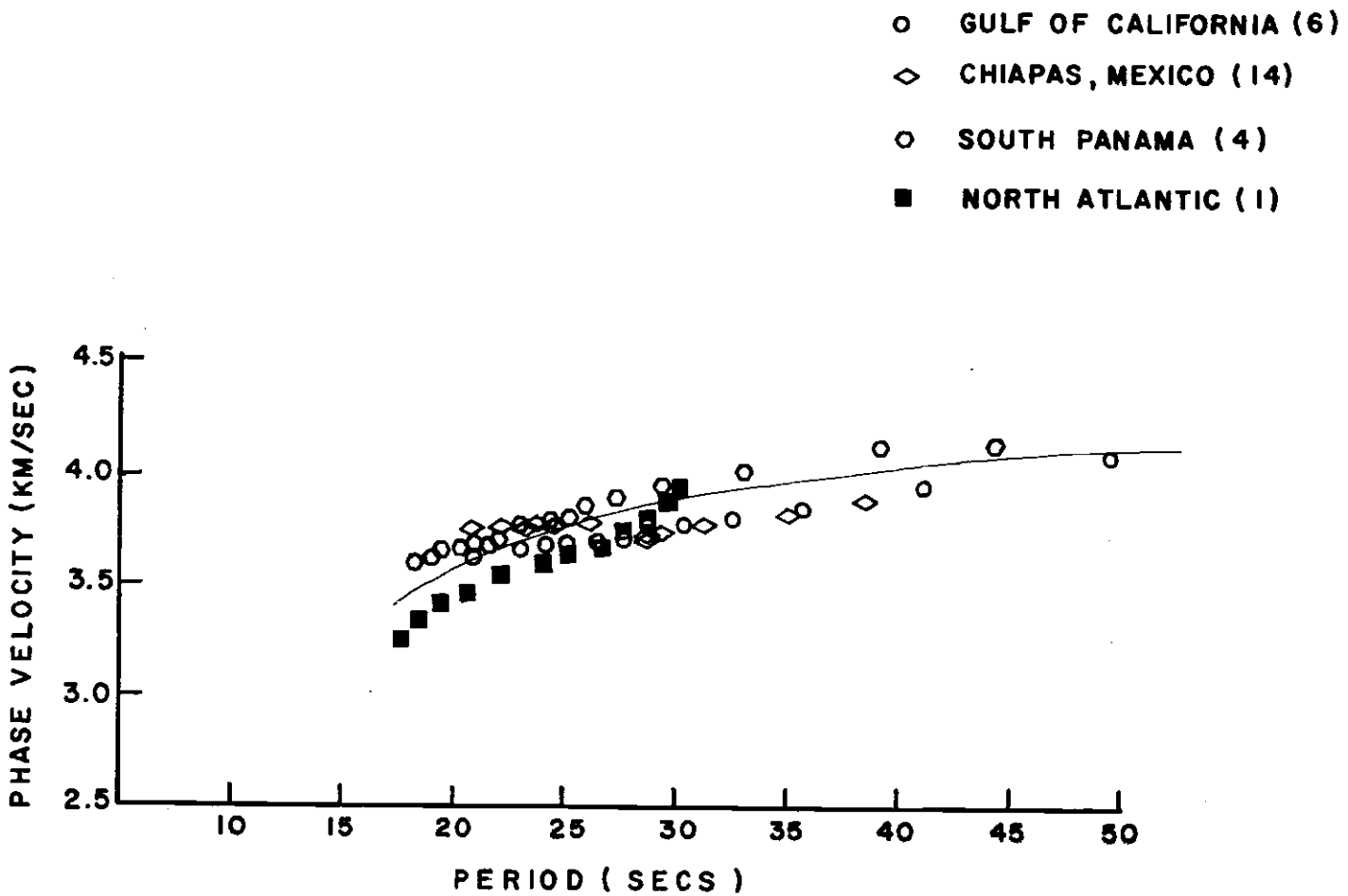

Figure 10. Composite Curve for Phase Velocities of Rayleigh Waves for Line Segment SHA-ATL-BLA.

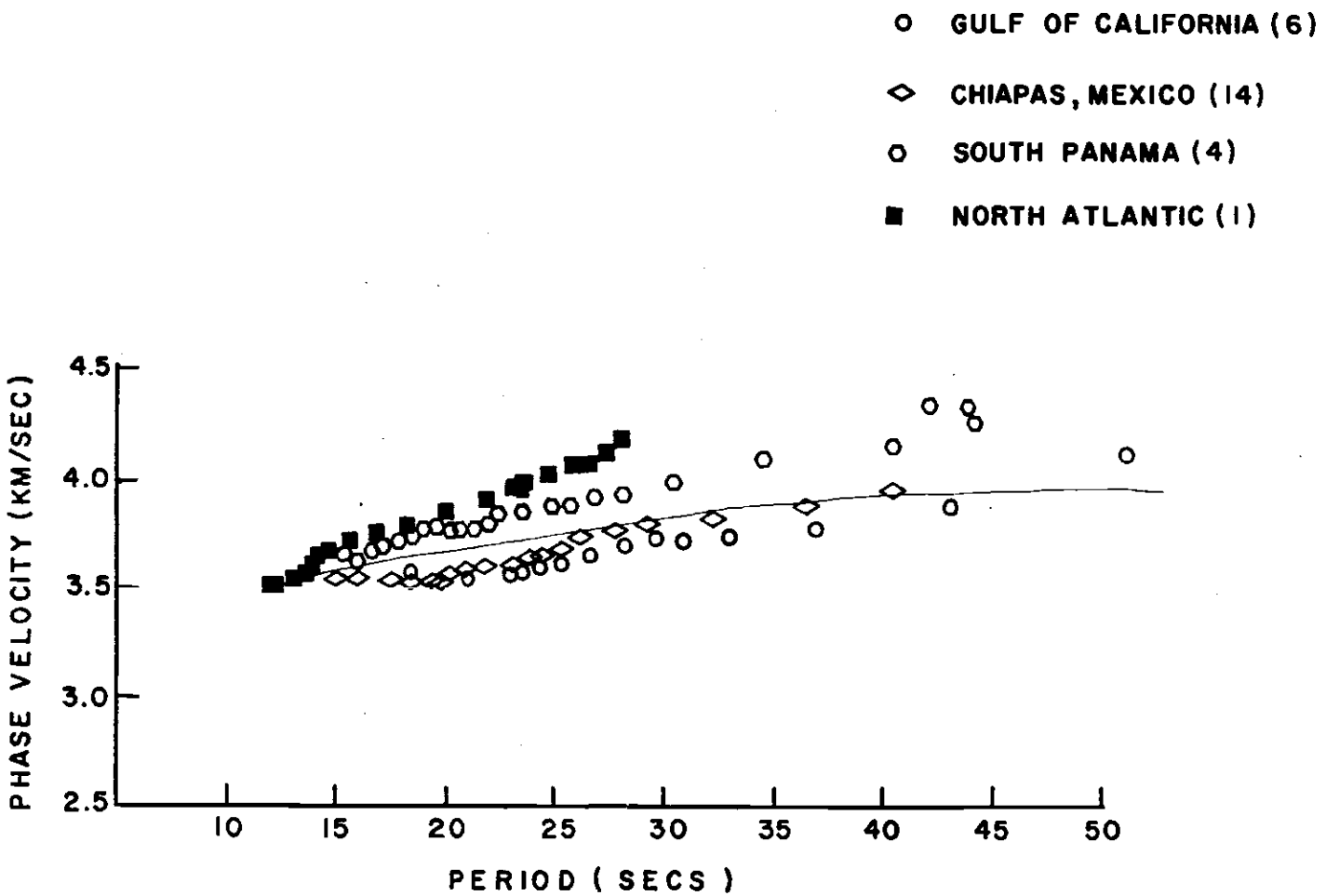

Figure 11. Phase Velocities of Rayleigh Waves Between ATL-BLA.

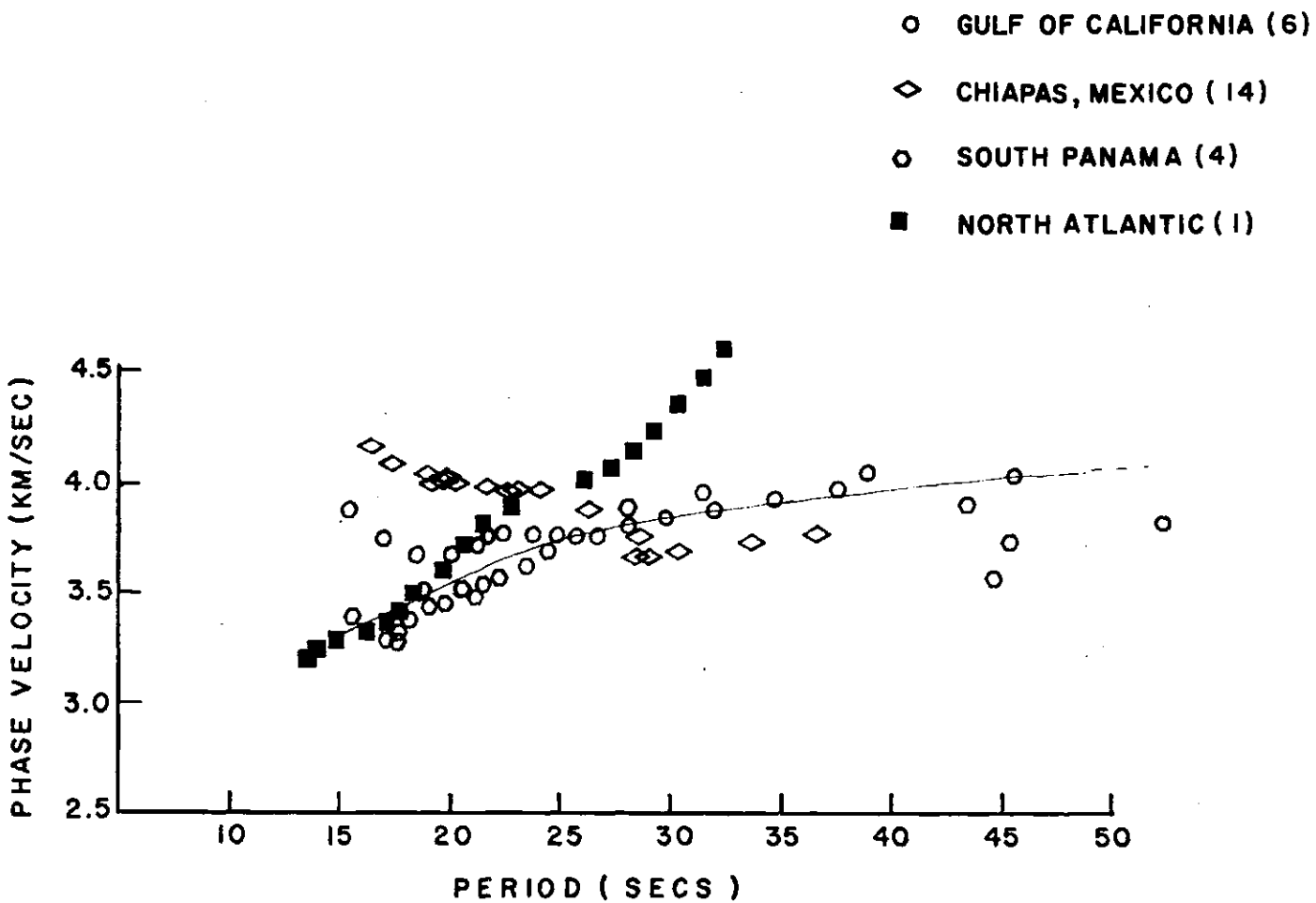

Figure 12. Phase Velocities of Rayleigh Waves Between ATL-SHA.

SHA, ATL, BLA fall along a straight line. However, in the case of event 1, from the North Atlantic, a new epicenter, displaced southwest of the original one by about 22 degrees gives more realistic velocities, but with an increase of velocity errors by 6 percent. For the California earthquake the surface waves travel essentially a continental path and hence there is no significant amount of refraction to affect the phase velocities.

The observed phase velocity dispersion for the four earthquakes was compared with theoretical curves. The lower line segment shows some scatter at higher frequencies largely due to interference. The curves for the upper line segment and that for the composite of four events compare very well and indicate that the crustal thickness along SHA-ATL-BLA lies between 35 km to 40 km, which is about 5 to 6 km less than that to be expected in the entire region of Southeast United States. This is probably because of the proximity of the Atlantic Coast, where the root of the Appalachian Mountains is shallower.

Phase Velocity of Rayleigh Waves Within the Upper Triangular Array (ATL-OXF-BLA).

The long period vertical component seismograms of the two earthquakes, 10 and 14, recorded at ATL, OXF, and BLA were utilized for finding the phase velocities as a function of period within the array. The Rayleigh waves from earthquake 10 (Leeward Islands), strike the North American Continent almost at right angles (Figure 4), so the possibility of curvature of wave front caused by refraction effects is minimized. This can clearly be seen from the data, because the minimum deviations for "false" epicenters "zero in" at the true epicenter. Phase velocity errors (0.39 km/sec) obtained are a little high but remarkably consistent for the

chosen periods. At short periods, 18-20.5 secs the false epicenter data are only slightly higher than that of the true epicenter and between 21 sec and 26 sec there is no difference at all. For periods greater than 30 seconds the data are too scarce to give any reliable information.

The surface waves from Chiapas, Mexico (14) strike the continent at an angle, whereby waves with shorter periods (18 secs-27 secs) undergo sharp refraction. The waves with longer periods (>30 sec), traveling at higher lower-crustal or upper-mantle velocities, are not affected very much. By applying the false epicenter technique, the new epicenter appears to be displaced to the East. This causes the lowering of phase velocities, because the Rayleigh waves, after refracting at the continental boundary, travel a longer refracted path at much slower continental velocities. The focused dispersion data, therefore, are more realistic and are thus used to find a crustal model for the upper triangle (see Figures 13 and 14).

The phase velocity dispersion data appears to be consistent with model No. 5 which has three crustal layers and a total thickness of 39 km.

Phase Velocity of Rayleigh Waves Within the Lower Triangular Array (ATL-OXF-SHA).

The dispersion data obtained from the three events with code numbers 3, 13, and 14 are shown in Figures 15 and 16. Earthquake 3, from the Kurile Islands, gives low velocity errors of 0.35 km/sec between the period ranges of 28-38 seconds. At other frequencies the errors are very large and hence the results are unreliable.

The shorter period surface waves traveling from South Sandwich Islands ($\approx 16{,}500$ km) show a large amount of scatter as mentioned previously, but the longer period phases arrive undisturbed. Therefore,

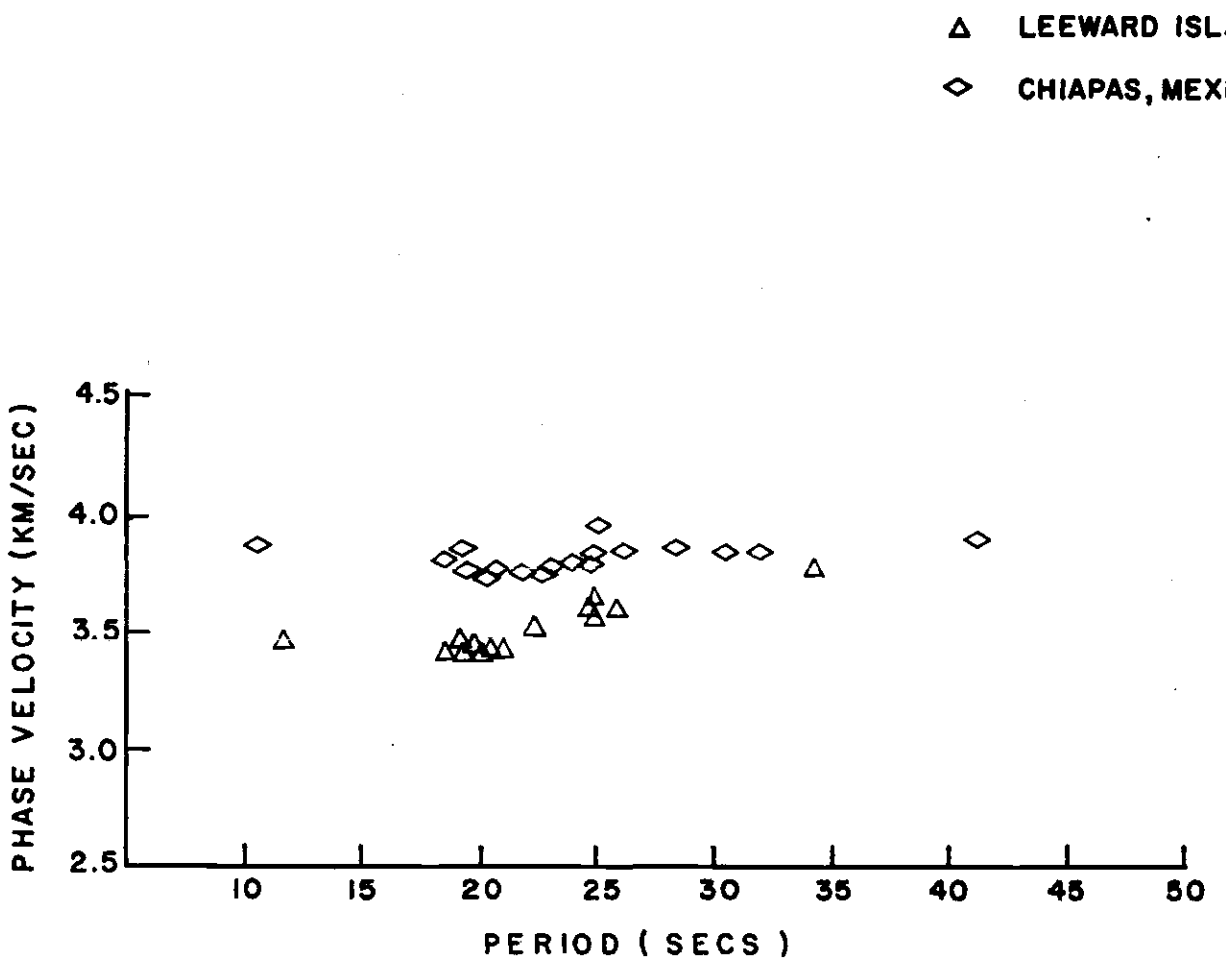

Figure 13. Phase velocities of Rayleigh Waves Within the Triangle ATL-BLA-OXF.

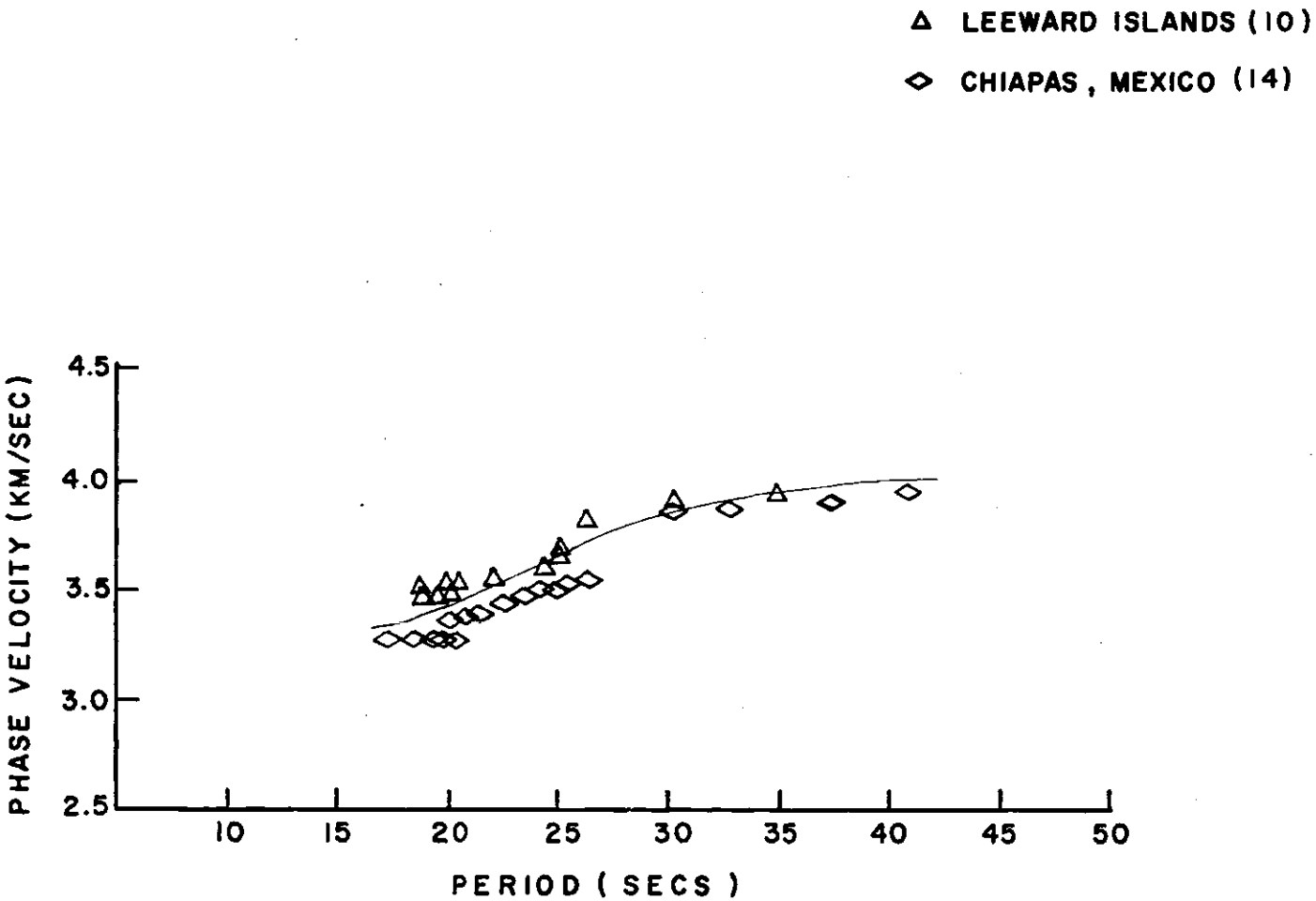

Figure 14. Phase Velocities of Rayleigh Waves, after Correcting for Refraction, Within Triangle ATL-BLA-OXF.

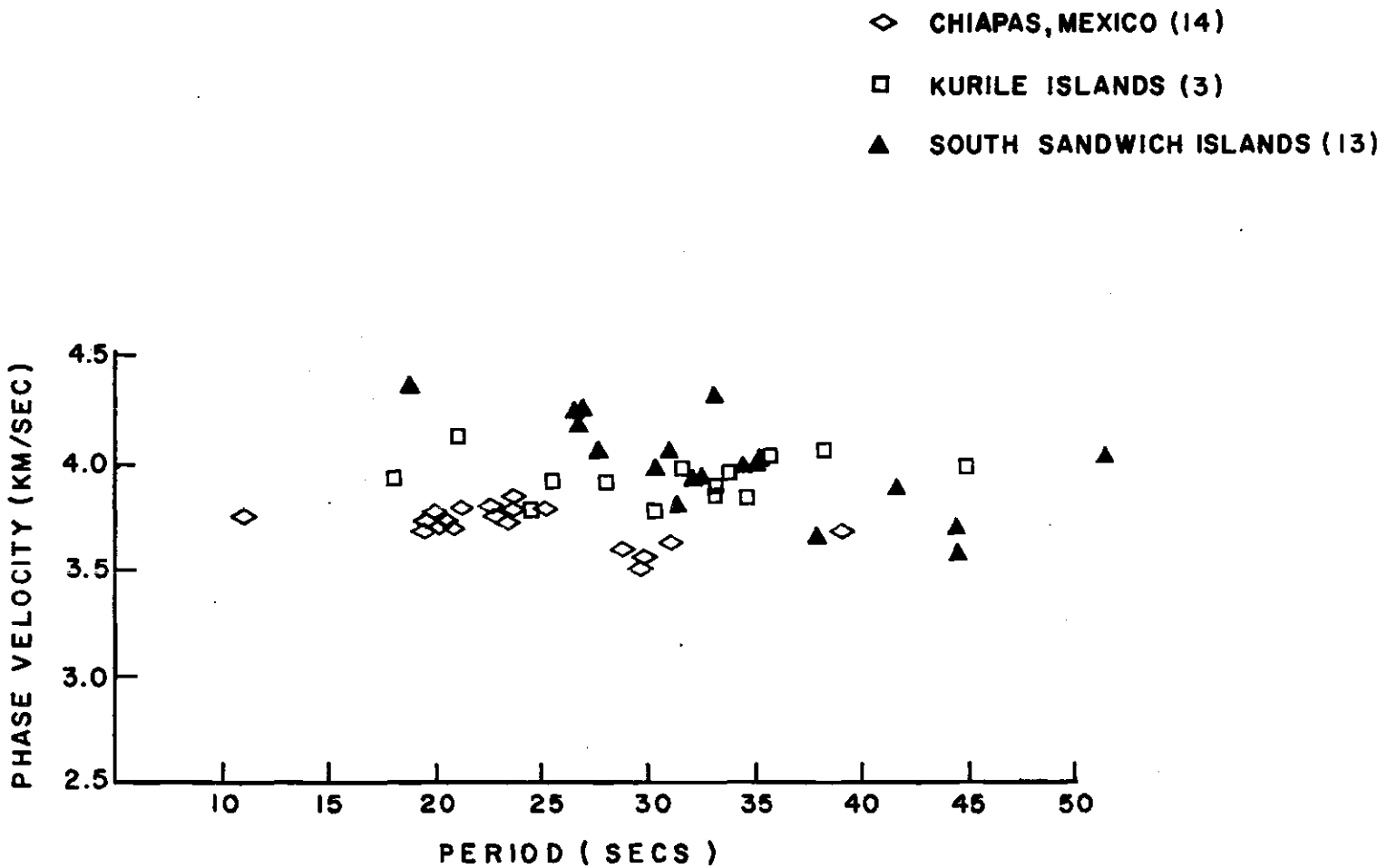

Figure 15. Phase Velocity of Rayleigh Waves Within the Triangle ATL-OXF-SHA.

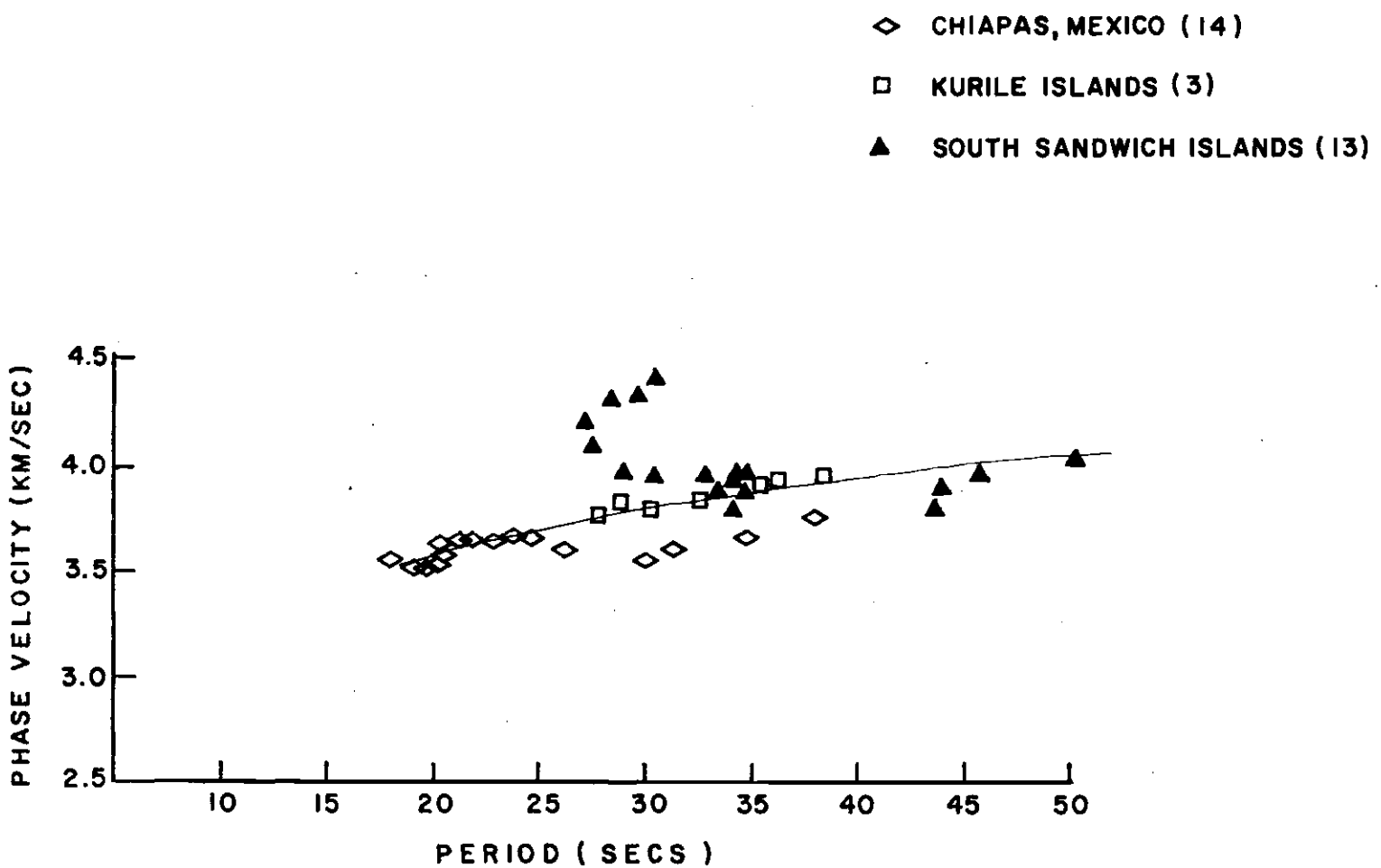

Figure 16. Phase Velocities of Rayleigh Waves, after Correcting for Refraction, Within Triangle ATL-OXF-SHA.

shorter periods are discarded from the final interpretation.

The data from the Mexico earthquake (14) indicate that between the period range of 38 to 30 seconds the epicenter does not shift and gives good results. However, for the periods between 28 secs to 20 secs the epicenter appears to shift about 10^{o} to the West, and for even lower periods ($\leq$ 20 seconds) the epicenter shifts further West beyond the limit of calculated "false epicenters." As before, the data after correction for refraction give lower velocities. The final curve drawn fits several models but is most consistent with model No. 6. The crustal thickness of this model is 43 km and consists of three layers.

RESULTS AND CONCLUSIONS

The crustal models No. 7 and 8 produce theoretical dispersion which agrees with observed composite dispersion data, corrected for refraction (Figure 17) and observed composite data uncorrected (Figure 18) for refraction, respectively. The uncorrected velocities show scatter particularly at small periods (10 secs-20 secs) indicating the effects of refraction of wave fronts. The crustal thickness indicated by the two models is the same, but the vertical velocity distribution in the crustal layers differs. This is because No. 7 has four crustal layers with a very thin surface layer of 1.0 km and three thick layers, thereas No. 8 has five crustal layers, of which the upper four are relatively thin and are respectively 0.5 km, 0.5 km, 5.0 km and 5.0 km (Figure 19).

It is to be understood that the models proposed here are not the only possible fits to the data. Phase velocity dispersion curves (Figure 20) for a single crustal layer of thicknesses of 39 km and 45 km were computed from dispersion tables for Rayleigh waves (Mooney and Bolt, 1965). The ratio of the shear wave velocities for the single layer model is based on travel times of earthquakes and explosions (Appendix I). The dispersion curve for the crustal depth of 39 km is in good agreement with the observed dispersion curves. However, in the period range of 25 to 35 seconds the observed data diviate from the theoretical single crustal layer dispersion curve indicating the presence of higher velocities in the lower crust. The velocity structure in models No. 7 and 8 confirm this conclusion.

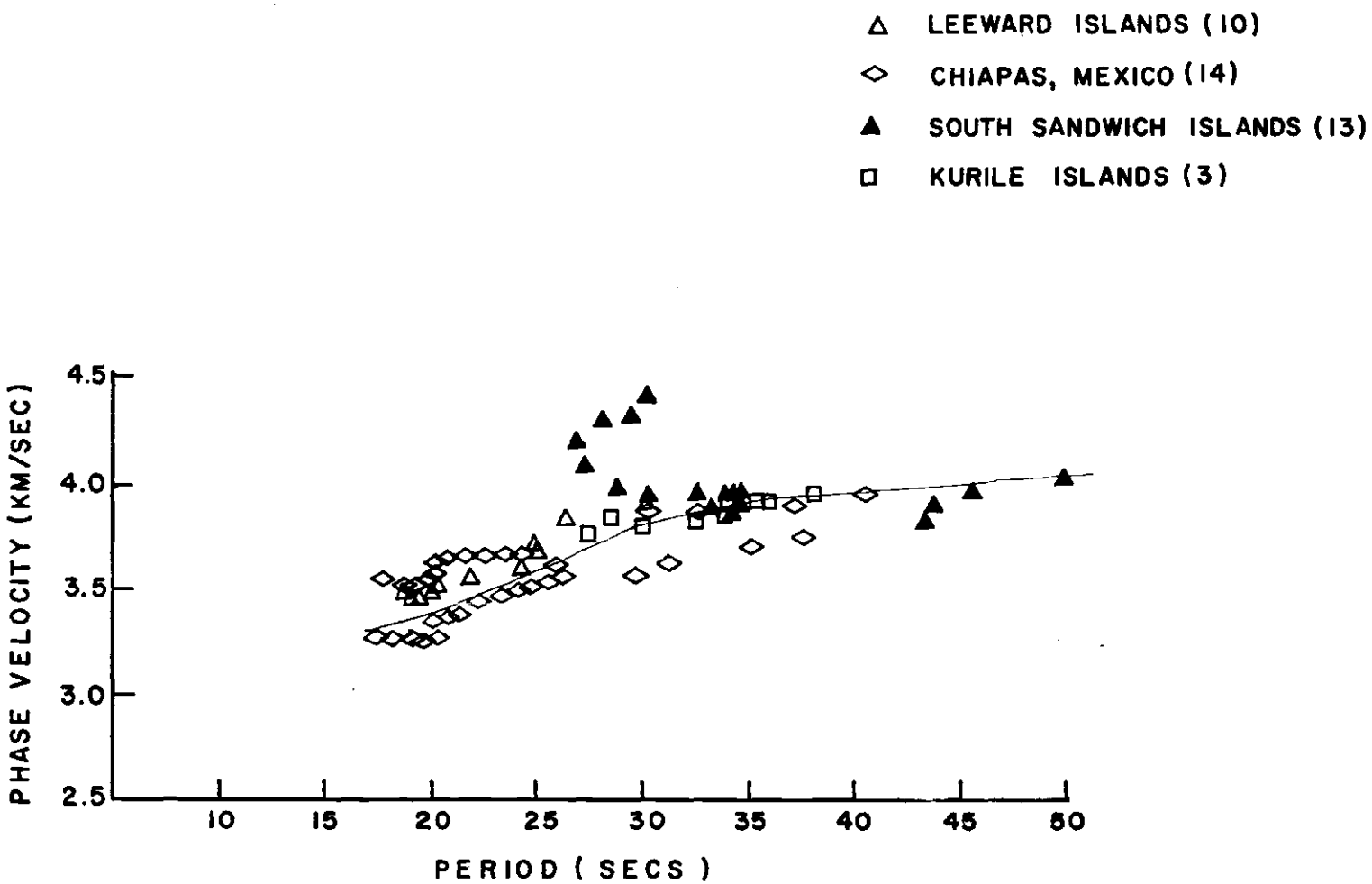

Figure 17. Composite Phase Dispersion Data, Corrected for Refraction, for Both Upper Triangle (ATL-BLA-OXF) and Lower Triangle (ATL-OXF-SHA).

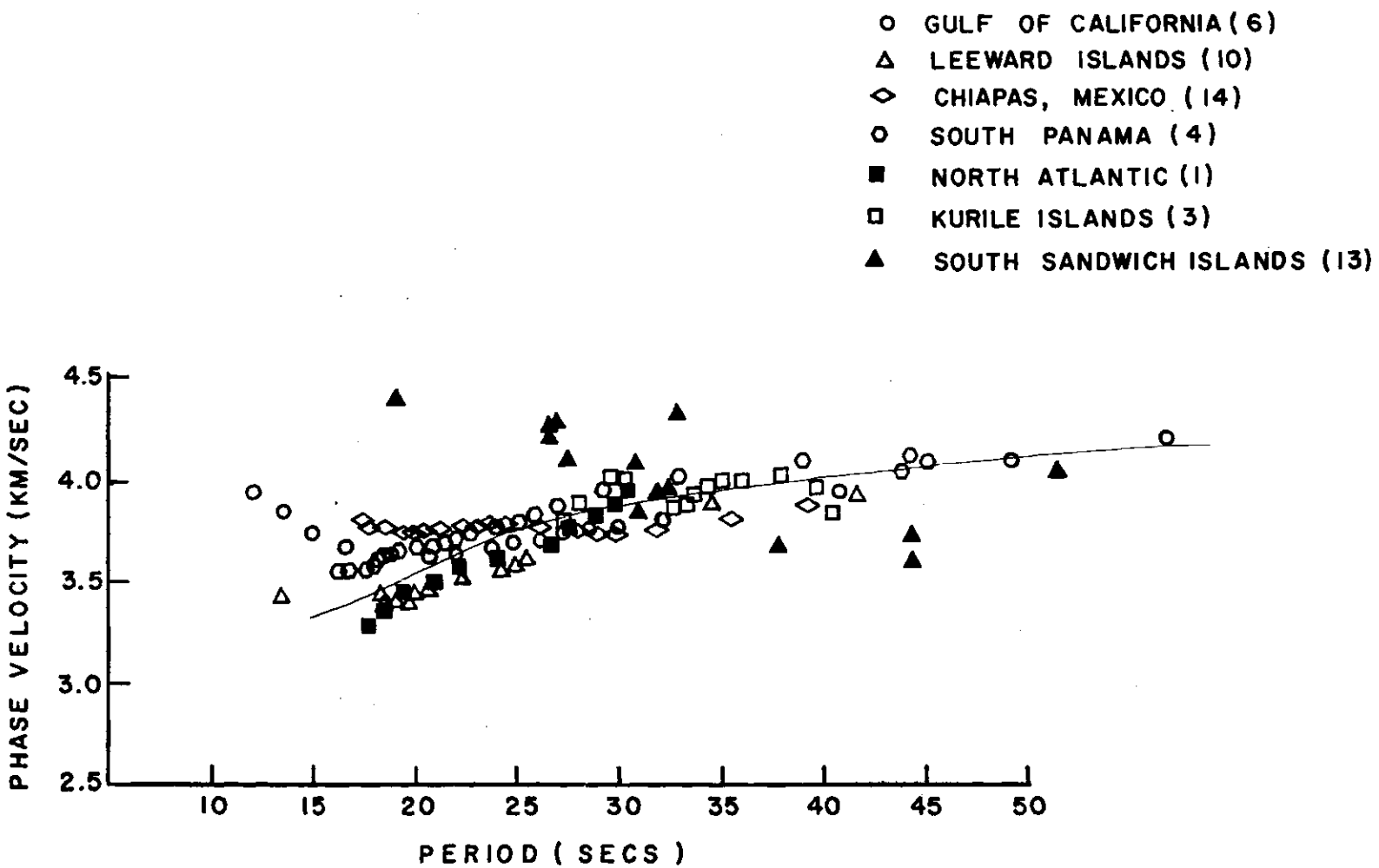

Figure 18. Composite Phase Dispersion Data from Seven Events.

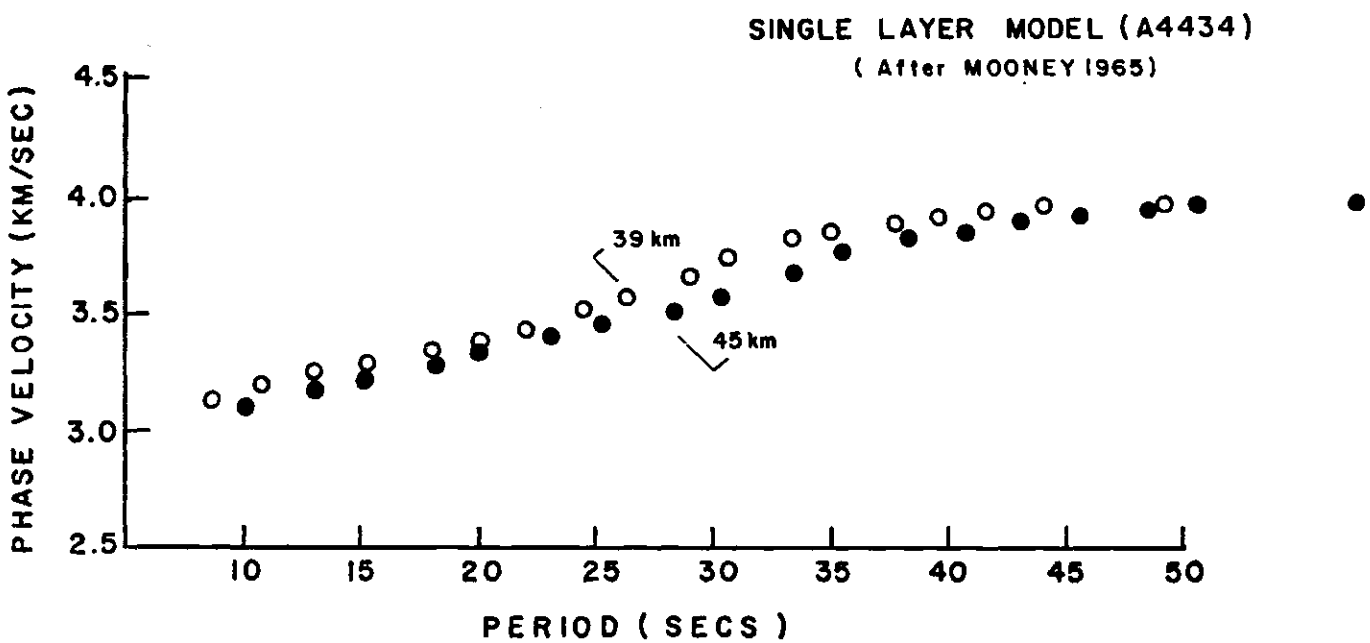

Figure 19. Vertical Shear Wave Velocity Distribution for the Models No. 7 and No. 8.

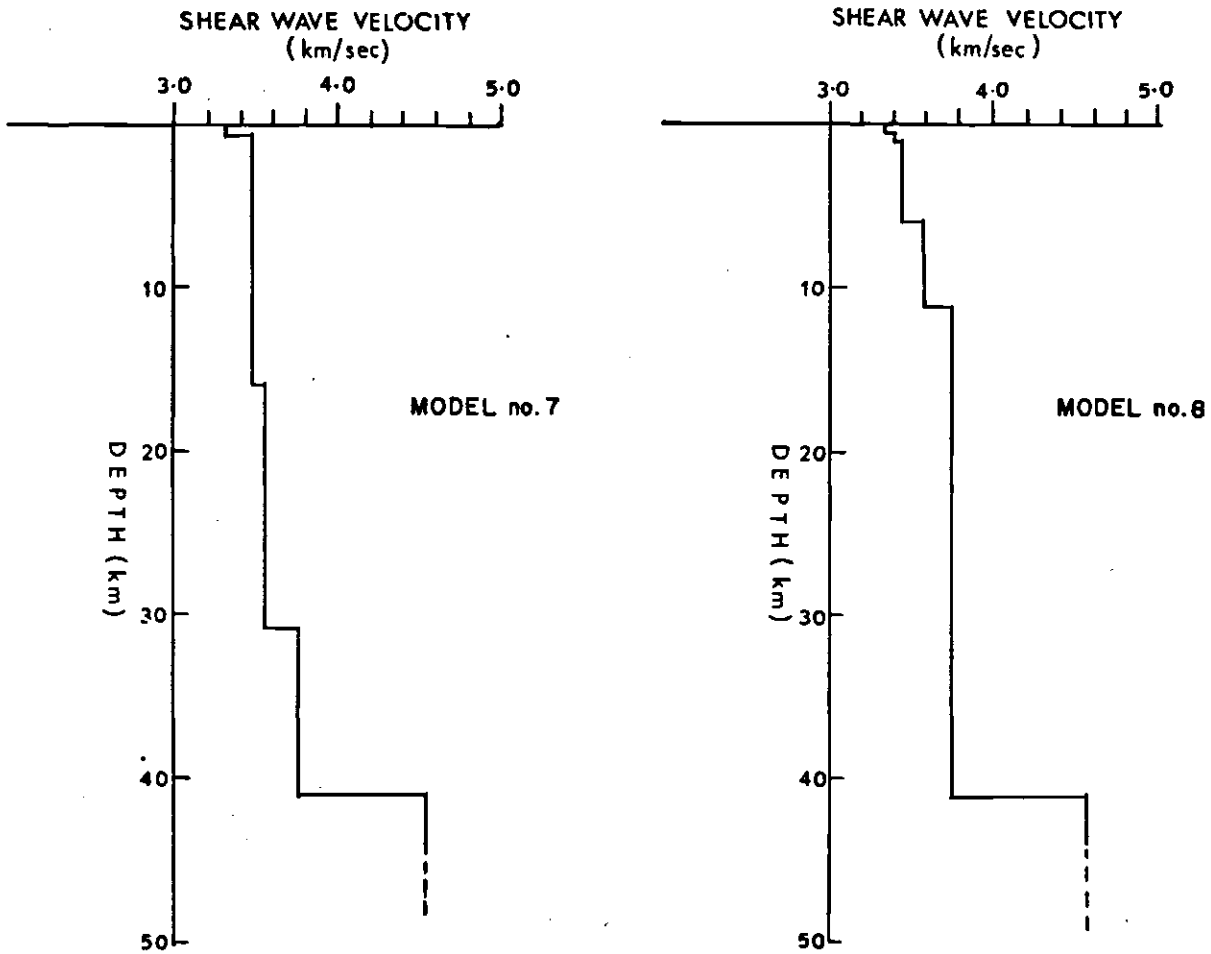

Figure 20. Theoretical Phase Velocity Dispersion of Rayleigh Waves for a Single Layer.

This investigation indicates that no extensive low-velocity layers exist within the crust sampled by this data. Nevertheless, the possibility remains that relatively thin low-velocity layers could occur. If the velocity of a thin layer is only slightly smaller than that of the overlying layer, its effects on dispersion could not be detected within the accuracy of these data. In general, the data indicate a higher velocity in the lower crust but are not precise enough to determine its depth or distinguish it from a gradational increase in velocity with depth.

Crustal model No. 7 supports the results of the refraction work done by Warren et al. (1966) in southern Mississippi and the interpretation by Tatel et al. (1953) of the T.V.A. shots fired at south Holston Dam in Tennessee. The crustal thickness of 41 km is consistent with that at Ansley (41 km, Figure 2), but definitely not with that at Raleigh (29 km). This probably indicates that the "hinge line" of the Appalachian mountains falls between Raleigh and Ansley. The lower crustal and upper mantle velocities of the final model are lower than the ones at McNeill and Collins. The crustal thickness of 45 km, mean crustal velocity of 6.57 km/sec and the upper mantle velocity of 8.06 km/sec at south Holston Dam compare quite well with the final chosen crustal model.

Slightly higher crustal thickness in eastern Tennessee and very low thickness at Raleigh and other variations in crustal velocities cannot be resolved with dispersion data alone. It should be combined with seismic refraction analysis for a more thorough investigation. This might even help in evaluating finer variations in crustal structures within one geologic province and also account for errors in phase velocity dispersion data apart from the effects of curvature, interference with higher modes

(frequencies) and effects of filtering.

The section in Figure 21 shows that the crust can be represented adequately by four layers, each of higher velocity than overlying layer (model No. 7). As it has been fairly well established by the dispersion data, this model can be extended horizontally to the eastern edge of the Appalachian mountains where the crustal thickness is slightly lower (35 km to 40 km). On this basis, the depth to the Mohorovicic discontinuity is found to range between 38 km and 42 km for the area under investigation in the southeastern United States.

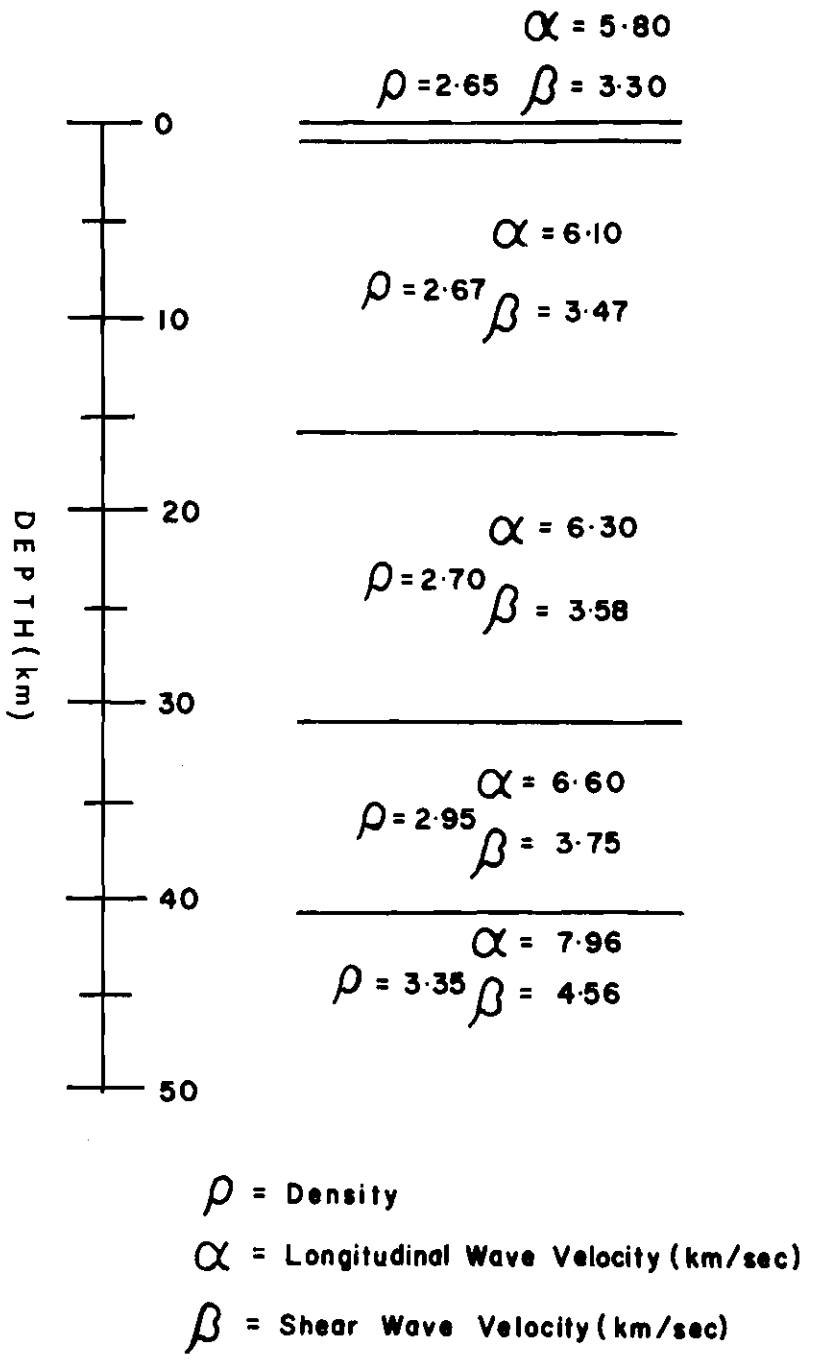

Figure 21. Crustal Model Proposed for the Area of Investigation in the Southeastern United States.

BIBLIOGRAPHY

BIBLIOGRAPHY

Bollinger, G. A. (1970) Travel-time study of six Central Appalachian earthquakes (1962-1968), Bull. Seis. Soc. Amer., vol. 60, pp. 629-637.

Bonini, W. E. (1957) Subsurface geology in the area of the Cape Fear Arch as determined by seismic refraction measurements, Ph.D. thesis, Univ. of Wisconsin, Madison.

Bonini, W. E. and G. P. Woolard (1960) Subsurface Geology of North Carolina-South Carolina Coastal Plain From Seismic Data. Bull. Am. Assoc. Petrol. Geol., vol. 44, pp. 298-315.

Bullen, K. E. (1963) An introduction to the theory of seismology, 3rd ed., Cambridge Univ. Press.

Chiburis, E. F. (1965) Crustal Structure in the Pacific Northwest states from phase-velocity dispersion of seismic surface waves, Ph. D. thesis, Oregon State Univ.

Dorman, J. (1962) Period equation for waves of Rayleigh type on a layered, liquid-solid half space, Bull. Seis. Soc. Amer., vol. 52, pp. 389-397.

Drake, C. L., M. Ewing and G. H. Sutton (1959) Continental margins and geosynclines: The east coast of North America north of Cape Hatteras, Physics and Chemistry of the Earth, vol. 3, Pergamon Press, pp. 110-198.

Eardley, A. J. (1962) Structural Geology of North America, Harper and Row, New York and Evanston.

Evernden, J. F. (1953) Direction of approach of Rayleigh waves and related problems. Part I., Bull. Seis. Soc. Amer., vol. 43, pp. 335-374.

Evernden, J. F. (1954) Direction of approach of Rayleigh waves and related problems. Part II., Bull. Seis. Soc. Amer., vol. 44, pp. 159-184.

Ewing, M. and F. Press (1950) Crustal structure and surface wave dispersion, Bull. Seis. Soc. Amer., vol. 40, pp. 271-280.

Ewing, M. and F. Press (1952) Crustal structure and surface wave dispersion. Part II. Solomon Islands earthquake of 29 July, 1950, Bull. Seis. Soc. Amer., vol. 42, pp. 315-325.

Gutenberg, B. (1924) Das Erdbeben in der chilenischen Atacama am 10 November 1922., Veroeffencl. Reichsanstalt Erdbebenforsch., vol. 3, pp. 29-48.

Hales, A. L., Helsley, C. E., Dowling, J. J., Nation, J. B. (1968) The East Coast On Shore-Off Shore Experiment - Part 1, The first arrival phases, Bull. Seis. Soc. Amer., vol. 58, pp. 757-819.

Harsey, J. B., E. T. Bunce, R. F. Wyrick, and F. T. Dietz (1959) Geophysical investigation of the continental margin between Cape Henry, Virginia and Jacksonville, Florida, Bull. Geol. Soc. Amer., vol. 70, pp. 437-466.

Haskell, N. A. (1953) The dispersion of surface waves in multilayered media, Bull. Seis. Soc. Amer., vol. 43, pp. 17-34.

King, P. B. (1959) The evolution of North America, Princeton Univ. Press.

Kinney, D. M. (Ed.). (1967) Basement Map of North America, Am. Assoc. Petrol. Geol. and United States Geological Survey.

Meyer, R. P. (1955) Seismic studies of off-shore geologic structure between Charleston, South Carolina and Cape Fear, North Carolina (abstract), Bull Geol. Soc. Amer., vol. 66, p. 1597.

Mooney, Harold M., Bolt, Bruce A. (1965) Dispersion tables for Rayleigh waves on a single surface layer. VESIAC Special Report, 4410-102-X, Institute of Science and Technology, The Univ. of Michigan.

Payo, G. (1965) Iberian Peninsula crustal structure from surface waves dispersion. Bull. Seis. Soc. Amer., vol. 55, pp. 727-743.

Press, F., M. Ewing, and J. Oliver. (1956) Crustal structure and surface wave dispersion in Africa. Bull. Seis. Soc. Amer., vol. 46, pp. 97-103.

Press, F. (1956) Determination of crustal structure from phase velocity of Rayleigh waves. Part I. Southern California, Bull. Geol. Soc. Amer., vol. 67, pp. 1647-1658.

Shapiro, R. (1970) Smoothing, filtering and boundary effects, Reviews of Geophysics and Space Physics, vol. 8, pp. 359-388.

Skeels, D. C. (1950) Geophysical data on North Carolina Coastal Plain, Geophysics, vol. 15, p. 409.

Steinhart, John S. and Robert P. Meyer. (1961) Explosion Studies of Continental Structure, Carnegie Inst. Publ., p. 409.

Tatel, H. E., L. H. Adams, and M. A. Tuve. (1953) Studies of the earth's crust using waves from explosions, Proc. Amer. Phil. Soc., vol. 97, pp. 658-669.

Tatel, H. E. and M. A. Tuve. (1955) Seismic exploration of a continental crust, in Crust of the Earth (Poldervaart, ed.), Geol. Soc. Amer., Spec. Paper 62, pp. 35-50.

Tuve, M. A., H. E. Tatel, and P. J. Hart. (1954) Crustal structure from seismic exploration, Jour. Geophys. Res., vol. 59, pp. 415-422.

Warren, D. H., J. H. Healy, W. H. Jackson. (1966) Crustal seismic measurements in southern Mississippi, Jour. Geophys. Res., vol. 71, pp. 3437-3456.

Wilson, J. T. and O. Baykal. (1948) Crustal Structure of the North Atlantic basin as determined from Rayleigh wave dispersion, Bull. Seis. Soc. Amer., vol. 38, pp. 41-53.

APPENDICES

APPENDIX I

CRUSTAL STRUCTURE STUDY OF SOUTHEASTERN UNITED STATES USING TRAVEL TIME DATA

Introduction

The seismic refraction method is one of the most powerful techniques available for the study of the compressional wave distribution with depth. This method relies on the use of travel times of first arrivals from artificial explosions and earthquakes. In this study seismograms of five quarry blasts with known origin times and four nearby earthquakes were analyzed. The quarry explosions in Georgia used in this study occurred: May 6 , 1965 at Gray, April 16, 1965 at Norcross, April 1, 1965 at Douglasville, February 18, 1965 at Red Oak, and February 19, 1965 at Stockbridge. The four earthquakes occurred: October 23, 1967 in South Carolina, December 13, 1969 in North Carolina, February 18, 1964 near North Georgia-Alabama border, and November 20, 1969 in West Virginia. The details on origin time, distance, P and S arrival times are listed in Charts I and II. Three recording stations (ATL, CPO and CHC) were used. The layers were assumed horizontal, since no reverse profiles were available.

Travel-Time Study Results

The first compressional wave arrivals in the distance range of 100 km to 460 km were observed from the four earthquakes and plotted on a travel time curve. The inverse of the slope of the line gave the

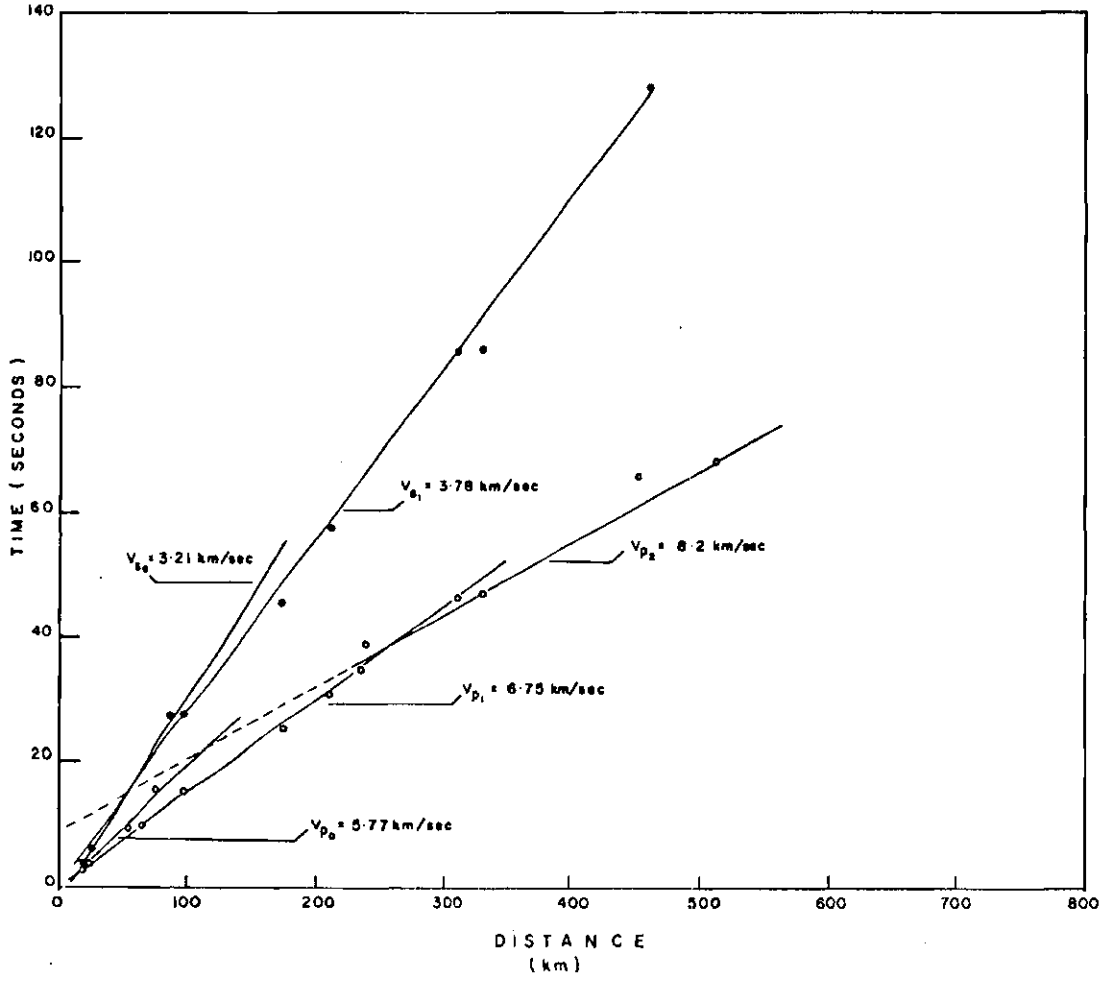

Travel Time Curves Showing P Wave and S Wave Velocities in the Area.

Chart I

Information on Quarry Blasts Recorded at ATL

No.	Date	Location	Distance (km)	Origin Time	P Arrival Time	P Travel Time	S Arrival Time	S Travel Time
1.	May 6, 1965	Gray, Ga.	88.80	23:24:59.66	23:25:15.5	15.84 sec	22:25:27.0	28.34 sec
2.	Apr. 16, 1965	Norcross, Ga.	59.2	21:44:02.99 17.20:12.77	21:44:12.36 17:20:29.7	9.37 sec		
3.	Apr. 1, 1965	Douglasville, Ga.	52.8	21:09:59.61	21:10:08.5	8.89 sec	21:10:15.0	15.39 sec
4.	Feb. 18, 1965	Redoak, Ga.	26.0	17:35:47.16	17:35:51.2	4.04 sec	17:35:53.8	6.64 sec
5.	Oct. 22, 1964	Tyrone, Ga.	24.0		17:06:19.6		17:06:22.5	
6.	Feb. 19, 1965	Stockbridge, Ga.	18.4	21:54:15.0	21:54:15.0	2.77 sec	21:54:16.8	4.57 sec

Chart II

Information on Earthquakes Used in Travel Time Study

1) West Virginia, H = 01:00:09.0; November 20, 1969

Station	Phase	Arrival Time	Travel Time (secs)	Distance (km)
CPO	P_n	01:01:15.2	66.2	458.3
	S_n	01:02:13.9	124.9	458.3
CHC	P_n	01:00:48.6	39.6	239.0
ATL	P_n	01:01:24.5	75.5	536.7

2) South Carolina, H = 09:04:10.1; October 23, 1969

Station	Phase	Arrival Time	Travel Time (secs)	Distance (km)
CPO	EP	09:05:18.5	68.4	506.0
CHC	EP	09:04:56.6	46.5	308.0
	IS	09:05:35.5	85.4	308.0
ATL	EP	09:04:57.3	47.2	330.0
	IS	09:05:36.5	86.4	330.0

Chart II - continued

3) Alabama, H = 09:31:11.6; February 18, 1964

Station	Phase	Arrival Time	Travel Time (secs)	Distance (km)
CPO	IP	09:31:27.2	15.6	99.0
CHC	ES	09:31:39.8	28.2	583.0
	EP	09:32:34.5	82.9	583.0
ATL	P	09:31:37.2	25.6	176.0
	S	09:31:57.1	45.5	176.0

4) North Carolina, H = 10:19:34.31; December 13, 1969

Station	Phase	Arrival Time	Travel Time (secs)	Distance (km)
CPO	IP	10:20:09.0	34.69	234.0
CHC	EP	10:20:55.0	80.69	370.0
ATL	P	10:20:05.9	31.59	210.5
	S	10:20:31.9	57.59	210.5

velocity of 8.23 km/sec. From the quarry blasts in the distance range of 18.4 km to 100 km the first arrivals plotted gave points to which two straight lines were found to fit. The velocities calculated were 5.77 km/sec down to a depth of 5.3 km and 6.75 km/sec between 5.3 km and 40.0 km. Shear wave arrivals were also observed and are shown on the travel time curve. The data indicate a shear wave velocity of 3.21 km/sec down to 5.3 km and 3.78 km/sec between 5.3 km and 40 km.

APPENDIX II

COMPUTER PROGRAMS

Period, Adjusted Arrival-Time, Phase Velocity and Error Determination

This program computes the periods averaged for stations used, directly from the adjusted arrival time data. It then calculates phase velocities and estimated errors by Least Mean Squares for all periods measured. New epicenters are then generated and minimum deviations calculated at each, for certain chosen periods.

Input

Card 1, 2: Format (2F15.4, 5A6/2I5), latitude (in degrees) longitude (in degrees), label (name of location and date of shock)/ Number of stations, Number of phases.

Card 3: Format (I5) - station identification.

Card 4: Format (10F7.1) - arrival times of phases as read from seismogram; ten/card.

Output

Print

Label, Latitude, Longitude, Number of stations, Number of points

Label and station identification

Arrival times at each station

Title/Adjusted arrival times

Corrected arrival times

Distance, Azimuth and station name

Title/period, velocity and errors

Chosen period, actual period, index, error

Title/period, velocity and errors

Distance and Azimuth Calculation Assuming Spherical Earth

Subroutine "AZDEL" (ALAT, ALONG, BLAT, BLONG, DEL, AZ) computes the distances and azimuths between two points based on the Spherical Earth (Bullen 1963, p. 155).

Input

ALAT is Latitude in degrees of point A, measured + North from equator.

ALONG is Longitude in degrees of point A, measured + East from 0^{o}.

BLAT is Latitude in degrees of point B, measured + North from equator.

BLONG is Longitude in degrees of point B, measured + East of 0^{o}.

Output

DEL is distance between points A and B in degrees.

AZ is direction or Azimuth in degrees of point A from B relative to North.

Adjusting the Arrival Time Data

Subroutine RSM (U,N,S) smooths the arrival time data according to Shipero (1970).

Input

U is the time function.

N is the number of points.

S is the smoothing factor.

Output

U is the smoothed (adjusted) time function, according to

$$U_J = U_J + S/2 \cdot (U_{J-1} - 2U_J + U_{J+1})$$

Determination of Phase Velocities and Measures of uncertainty (Errors)

Subroutine (ERBLOK(K, NS, NP, VEL, C, ER) calculates phase velocities and errors by least mean squares using the mathematical expression as given by Bullen (1963 p. 196).

Input

K is the number of phases.

NS is the number stations.

NP is the number of phases.

Output

VEL is the phase velocity.

C is the constant.

ER is the minimum deviations in velocity.

```
      DIMENSION LABEL(10),TAU(100),ERROR(5,5),X(4),Y(4),LXY(4),
     1U(100)
      COMMON D(4),T(4,100),JSTA(4)
      DATA X/33.433,37.211,34.512,30.695/,Y/-84.338,- 80.421,-89.409,-
     188.140/,LXY/3HATL,3HBLA,3HOKF,3HSHA/
   10 READ(5,67,END=99) V,V,(LABEL(I),I=1,5),NS,NP
   67 FORMAT(2F15.4,5A6/2I5)
      DO 431 M=1,4
      DO 431 N = 1,100
      T(M,N) = 0.
  431 CONTINUE
      WRITE(6,68) (LABEL(I),I=1,5),V,V,NS,NP
   68 FORMAT(1H1,5A6,5X,2F15.4,5X,2I5)
      DO 21 IJ = 1,NS
      READ(5,34) JSTA(IJ)
      JST = JSTA(IJ)
   21 READ(5,35) (T(JST,K),K=1,NP)
   34 FORMAT (I5)
   35 FORMAT(10F7.1)
      WRITE(6,22) (LABEL(I),I=1,5),(LXY(I),I=1,4)
   22 FORMAT(1H1,5A6/4X,A6,4X,A6,4X,A6,4X,A6)
      DO 23 K=1,NP
   23 WRITE(6,24) (T(I,K),I=1,4)
   24 FORMAT(1X,4F10.1)
      DO 279 I = 1,NS
  277 JST = JSTA(I)
      DO 278 J = 1,NP
  278 U(J) = T(JST,J)
      DO 137 KK = 1,5
      CALL RSM(U,NP,-0.5)
      CALL RSM(U,NP,+0.5)
  137 CONTINUE
      DO 279 J = 1,NP
  279 T(JST,J) = U(J)
      WRITE(6,332)
  332 FORMAT(1H1,15X,22HADJUSTED ARRIVAL TIMES)
      DO 66 J = 1,NP
   66 WRITE(6,24) (T(JST,J),JST = 1,4)
      NP1 = NP-1
      DO 27 K=1,NP1
      TAU(K) = 0.
      DO  28 I=1,NS
      JST = JSTA(I)
   28 TAU(K) = T(JST,K+1)-T(JST,K)+TAU(K)
   27 TAU(K) = (TAU(K)*2)/NS
      DO 38 IX = 1,NS
      JST = JSTA(IX)
      CALL AZDLL (V,V,X(JST),Y(JST),D(JST),AZ)
      WRITE(6,100) D(JST),AZ,LXY(JST)
  100 FORMAT(10X,F10.6,10X,F10.6,5X,A6)
   38 CONTINUE
      WRITE(6,333)
  333 FORMAT(1H1,15X,7H PERIOD,10X,9H VELOCITY,8X,11H +OR- ERROR/
     113X,7H (SECS),10X,9H (KM/SEC),10X,7H (SECS) )
      DO 40 K=1,NP
      CALL ERRLOK(K,NS,NP,VEL,C,ER)
      WRITE(6,72) TAU(K),VEL,ER
      TAUK = TAU(K)*0.12
      VELP = VEL*1.2
   72 FORMAT(10X,F12.3,5X,F12.3,5X,F12.3)
   40 CONTINUE
C     CHOOSE PERIOD
      T2 = 50.
   71 CONTINUE
      T2 = T2-5.
      IF (T2.LE.15.) GO TO 10
      DO 41 K = 2,NP
      INDEX = K
      IF (TAU(K).LE.T2)  GO TO 73
```

```
   41 CONTINUE
   73 CONTINUE
      DO 108 LAT = 1,5
      DO 108 LONG = 1,5
      ERROR(LAT,LONG) = 0.
  108 CONTINUE
      SMALL = 0.99E+10
      ALAT = W - 30.
      DO 109 LAT = 1,5
      ALONG = V-30.
      ALAT = ALAT + 10.
      DO 109 LONG = 1,5
      ALONG = ALONG + 10.
      DO 117 IX = 1,NS
      JST = JSTA(IX)
      CALL AZDEL(ALAT,ALONG,X(JST),Y(JST),D(JST),AZ)
  117 CONTINUE
      CALL ERBLOK(INDEX,NS,NP,VEL,C,ER)
      ERROR(LAT,LONG) = ER
      IF (ER.GE.SMALL) GO TO 109
      SMALL = ER
      SLAT = ALAT
      SLONG = ALONG
  109 CONTINUE
      WRITE(6,61) T2,TAU(INDEX),INDEX,ERROR
   61 FORMAT(1X,2F10.2,I5//(5E15.2))
      DO 710 IX = 1,NS
      JST = JSTA(IX)
      CALL AZDEL(SLAT,SLONG,X(JST),Y(JST),D(JST),AZ)
  710 CONTINUE
      WRITE (6,333)
      DO 141 K = 1,NP
      CALL ERBLOK(K,NS,NP,VEL,C,EP)
      WRITE(6,72) TAU(K),VEL,ER
  141 CONTINUE
      GO TO 71
      CONTINUE
   99 STOP
      END
```

```
      SUBROUTINE RSM(U,N,S)
      DIMENSION U(100)
      U1 = U(1)
      U(1) = U(1) + S*(U(2)-U(1))
      NN = N-1
      DO 36 J = 2,NN
      U2 = U(J)
      J1 = J + 1
      U(J) = U(J) + S*(U1 + U(J1)-2*U2)/2.
   36 U1 = U2
      U(N) = U(N) + S*(U1-U(N))
      RETURN
      END

      SUBROUTINE AZDEL(ALAT,ALONG,BLAT,BLONG,DEL,AZ)
C      FINDS THE AZIMUTH AND DISTANCE FROM POINT B TO A.  ALL ANGLES IN
C     DEGREES. AZIMUTH FROM NORTH CLOCKWISE, LATITUDE IS NEGATIVE SOUTH,
C     LONGITUDE IS NEGATIVE WEST. SPHERICAL EARTH. BULLEN PG 155
      CF = 0.0174532925
      A = ALAT*CF
      B = BLAT*CF
      AB = (ALONG-BLONG)*CF
      DEL = COS(B)*COS(A)*COS(AB)+SIN(A)*SIN(B)
      DEL = ACOS(DEL)/CF
      X = COS(A)*SIN(AB)
      Y = SIN(A)*COS(B)-COS(A)*SIN(B)*COS(AB)
      AZ = ATAN2(X,Y)/CF
      IF(AZ)    24,25,25
   24 AZ = AZ+360
   25 RETURN
      END
```

```
      SUBROUTINE ERBLOK(K,NS,NP,VEL,C,ER)
      COMMON D(4),T(4,100),JSTA(4)
      CF = 0.0174532925
C FINDS THE VELOCITIES BY LEAST MEAN SQUARES AND CALCULATES ERRORS
      DSQ=0.
      DO 8 I=1,NS
      J=JSTA(I)
      DSQ = DSQ+(D(J)*D(J))
    8 CONTINUE
      DISQ = 0.
      DO 9 I=1,NS
      J=JSTA(I)
    9 DISQ = DISQ+D(J)
      DISQ = DISQ*DISQ
      DT = 0.
      DO 110 I=1,NS
      J = JSTA(I)
      DT = DT + D(J)*T(J,K)
  110 CONTINUE
      DTJ = 0.
      DO 11 I = 1,NS
      J = JSTA(I)
   11 DTJ = DTJ + D(J)
      SD =DTJ
      DJT = 0.
      DO 111 I = 1,NS
      J = JSTA(I)
  111 DJT = DJT + T(J,K)
      DTJ = DTJ*DJT
      DTSQ = DT*SD

      DISQT = DJT*DSQ
       VEL = ((NS*DSQ)-DISQ)/((NS*DT)-DTJ)
      C = (-DTSQ+ DISQT)/((NS*DSQ)-DISQ)
      ER = 0.0
      IF (NS.LE.2)  GO TO 21
      CONTINUE
      DO 311 I=1,NS
      J = JSTA(I)
  311 ER = ER + (D(J)/VEL+C-T(J,K))**2
      ER = ER/(NS-2)
      ER = SQRT(NS*ER/(NS*DSQ-DISQ))
   21 VEL = VEL*110.
      RETURN
      END
```

APPENDIX III

THEORETICAL DISPERSION CURVES AND VELOCITY MODELS

The models presented here are only the ones that fit the dispersion data for certain specified portions of the area of study. They were taken from Chiburis (1965) and were computed by Dorman's (1962) PV-7EF computer program. PV 7EF computes the phase and group velocity dispersion curves for all modes of Love and Rayleigh waves on an elastic half space of flat homogeneous layers by solution of a transcendental equation. The source language of this program is Fortran. The computation is based on Haskell's (1953) matrix integration method.

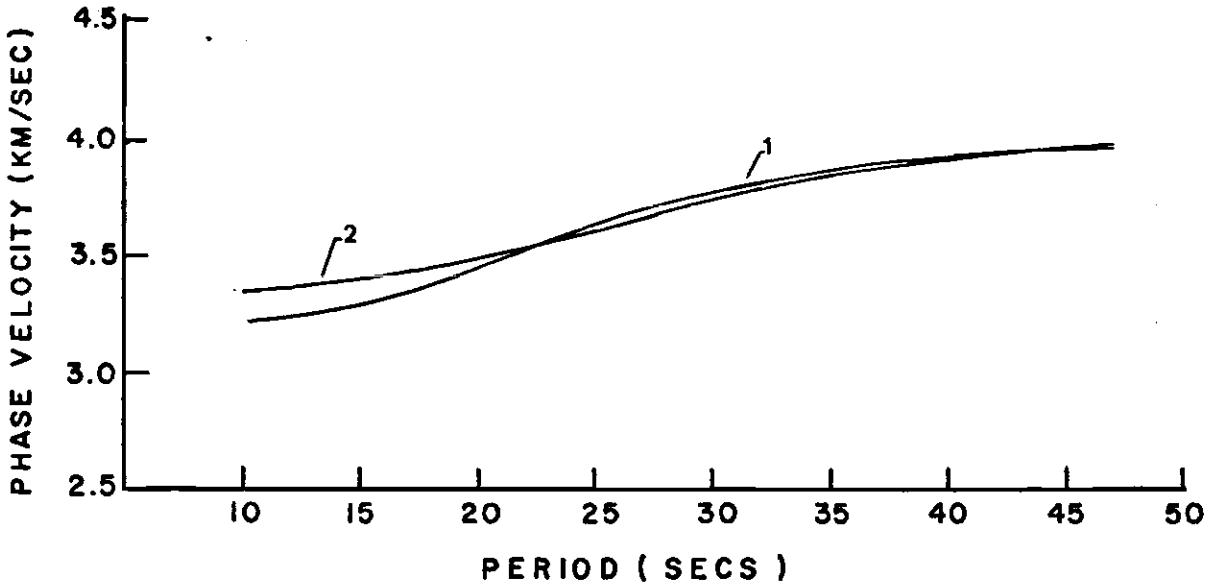
PHASE VELOCITY (KM/SEC)
4.5
4.0
3.5
3.0
2.5
10
15
20
25
30
35
40
45
50
PERIOD (SECS)
1
2

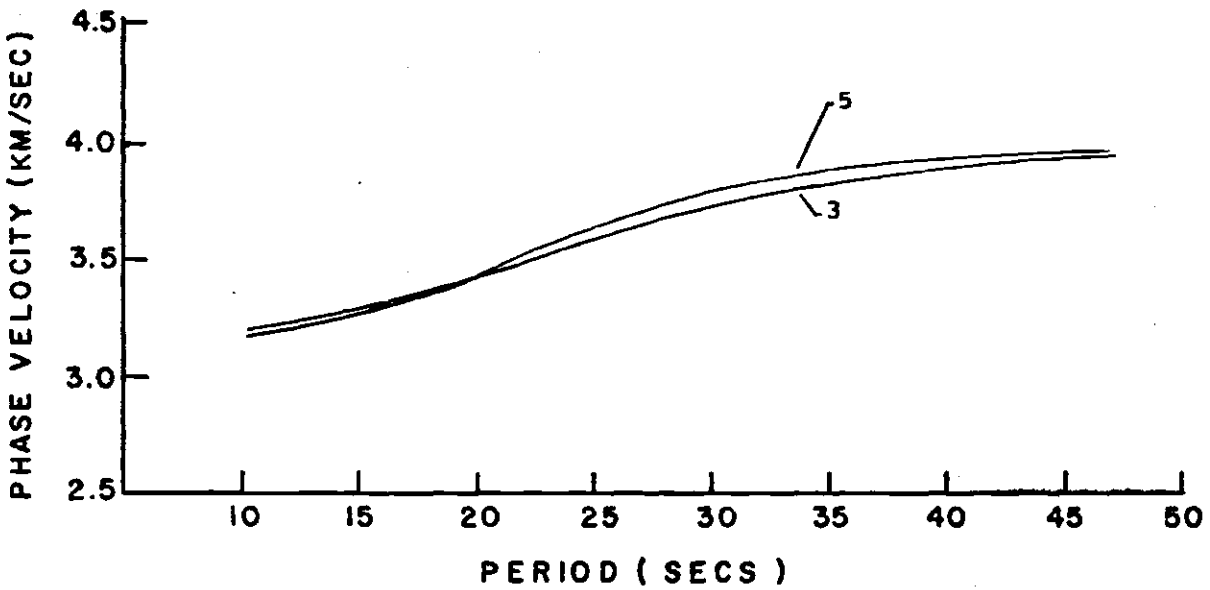
PHASE VELOCITY (KM/SEC)
4.5
4.0
3.5
3.0
2.5
10
15
20
25
30
35
40
45
50
PERIOD (SECS)
5
3

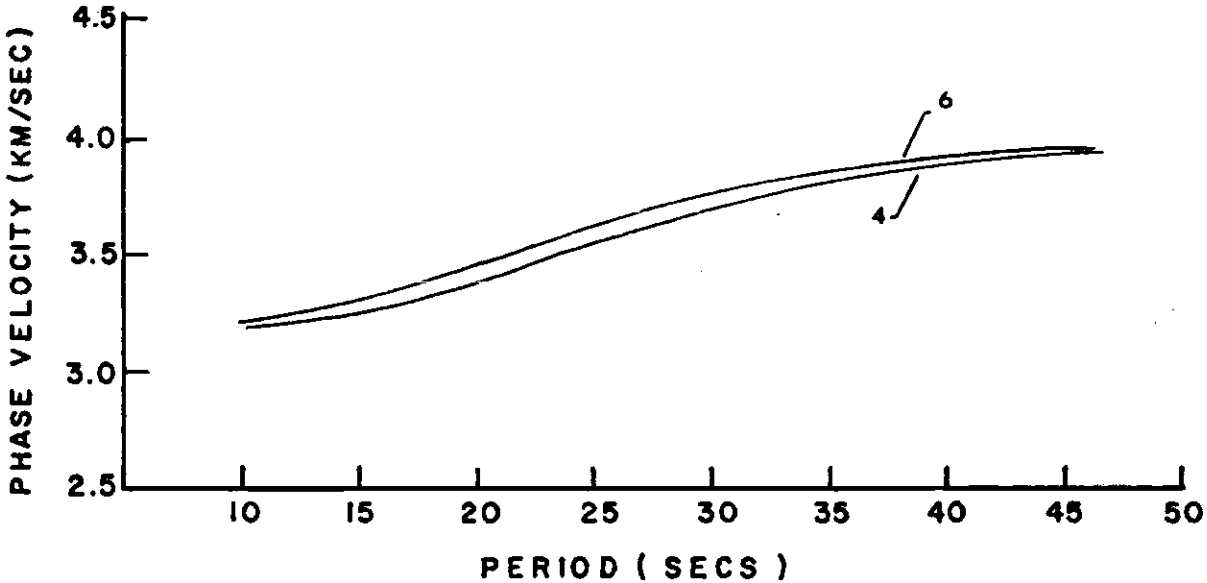
PHASE VELOCITY (KM/SEC)
4.5
4.0
3.5
3.0
2.5
10
15
20
25
30
35
40
45
50
PERIOD (SECS)
6
4

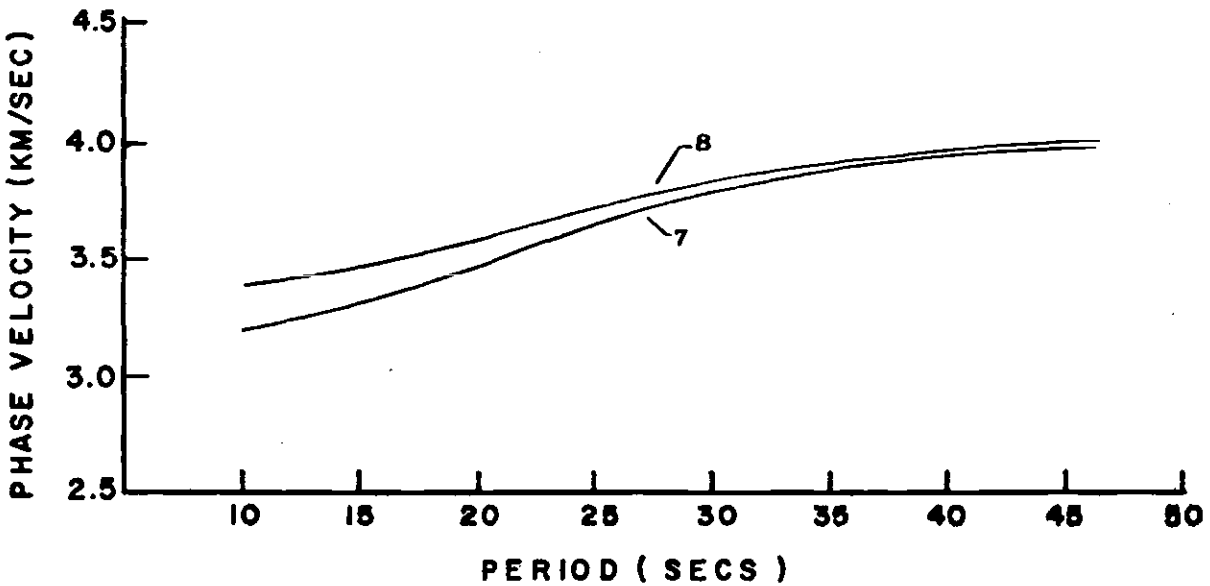
PHASE VELOCITY (KM/SEC)
4.5
4.0
3.5
3.0
2.5
8
7
10
15
20
25
30
35
40
45
50
PERIOD (SECS)

CRUSTAL MODELS

Thickness	Longitudinal Wave Velocity	Sheer Wave Velocity	Density	Crustal Model Number
5.0	5.53	3.15	2.70	
40.0	6.60	3.75	2.84	1
0	7.96	4.56	3.35	
15.0	6.10	3.45	2.67	
15.0	6.30	3.58	2.75	2
15.0	6.60	3.76	3.00	
0	7.96	4.56	3.35	
4.0	5.90	3.34	2.60	
0.5	6.00	3.40	2.67	
15.0	6.10	3.47	2.67	3
15.0	6.30	3.58	2.70	
10.0	6.60	3.75	2.95	
0	7.96	4.56	3.35	
4.0	5.90	3.36	2.67	
25.0	6.10	3.47	2.67	4
10.0	6.60	3.75	2.95	
0	7.96	4.56	3.35	
1.0	5.90	3.36	2.67	
22.0	6.10	3.47	2.67	5
20.0	6.60	3.75	2.95	
0	7.96	4.56	3.35	
1.0	5.80	3.30	2.65	
20.0	6.10	3.47	2.67	
10.0	6.30	3.58	2.70	6
10.0	6.60	3.75	2.95	
0	7.96	4.56	3.35	
1.0	5.80	3.30	2.65	
15.0	6.10	3.47	2.67	
15.0	6.30	3.58	2.70	7
10.0	6.60	3.75	2.95	
0	7.96	4.56	3.35	
0.5	5.90	3.34	2.67	
0.5	6.00	3.40	2.67	
5.0	6.10	3.45	2.67	8
5.0	6.30	3.58	2.70	
30.0	6.60	3.76	2.84	
0	7.96	4.56	3.35	